Kinetic Simulations of Neoclassical Transport in Tokamak Plasmas

E.A. Belli
General Atomics

Acknowledgements:
C. Angioni, J. Candy, F. Casson, C. Holland,
O. Meneghini, R. Nazikian, T. Osborne, P. Snyder

ITER International School
Aix en Provence, Aug 25-29, 2014

GENERAL ATOMICS

Neoclassical dynamics are believed to be important in explaining enhanced edge flows, current, and confinement in tokamaks.

- **Neoclassical transport** dominants over turbulence in regions of weak gradients and in transport barriers.
- Substantial **ion flow in the tokamak boundary region** can be important for the stabilization of instabilities and the radial transport of plasma.
- The **neoclassical bootstrap current** is known to be important for a steady-state reactor in which only a small fraction of the current can be driven externally.
- Intrinsic **toroidal plasma rotation due to the NTV** induced by 3D magnetic perturbations may be important for confinement in reactors, where the momentum input is small.

Outline

- **Overview of kinetic theory**
- **Drift-kinetic neoclassical simulations**
  - Numerical algorithms
  - Reduced models
- **Integrated modeling**
  - MHD equilibrium reconstruction
  - Steady-state transport
- **Advanced physics effects**
  - Strong toroidal rotation
  - Nonaxisymmetry
  - Nonlocal effects

Outline

- **Overview of kinetic theory**
- **Drift-kinetic neoclassical simulations**
  - Numerical algorithms
  - Reduced models
- **Integrated modeling**
  - MHD equilibrium reconstruction
  - Steady-state transport
- **Advanced physics effects**
  - Strong toroidal rotation
  - Nonaxisymmetry
  - Nonlocal effects

The Fokker-Planck equation provides the fundamental theory for plasma equilibrium, fluctuations, and transport.

$$\left[\frac{\partial}{\partial t}+\vec{v}\cdot\nabla+\frac{z_a e}{m_a}\left(\vec{E}+\hat{\vec{E}}\right)\cdot\frac{\partial}{\partial\vec{v}}+\frac{z_a e}{m_a c}\vec{v}\times\left(\vec{B}+\hat{\vec{B}}\right)\cdot\frac{\partial}{\partial\vec{v}}\right]\left(f_a+\hat{f}_a\right)=\sum_b C_{ab}\left(f_a+\hat{f}_a,f_b+\hat{f}_b\right)+S_a$$

$f_a,\vec{E},\vec{B}$ → ensemble-averaged

$\hat{f}_a,\hat{\vec{E}},\hat{\vec{B}}$ → fluctuating

- Separate into the eqn into **ensemble-averaged** and **fluctuating** components:

$$A=\left[\frac{\partial}{\partial t}+\vec{v}\cdot\nabla+\frac{z_a e}{m_a}\left(\vec{E}+\frac{\vec{v}}{c}\times\vec{B}\right)\cdot\frac{\partial}{\partial\vec{v}}\right]f_a-\left\langle C_a\right\rangle_{ens}-D_a-S_a=0 \rightarrow \textbf{DKE}$$

$$F=\left[\frac{\partial}{\partial t}+\vec{v}\cdot\nabla+\frac{z_a e}{m_a}\left(\vec{E}+\frac{\vec{v}}{c}\times\vec{B}\right)\cdot\frac{\partial}{\partial\vec{v}}\right]\hat{f}_a+\frac{z_a e}{m_a}\left(\hat{\vec{E}}+\frac{\vec{v}}{c}\times\hat{B}\right)\cdot\frac{\partial}{\partial\vec{v}}\left(f_a+\hat{f}_a\right)-C_a+\left\langle C_a\right\rangle_{ens}+D_a=0$$

→ **GKE**

Fluctuation-particle interaction op: $D_a=-\frac{z_a e}{m_a}\left\langle\left(\left(\hat{\vec{E}}+\frac{\vec{v}}{c}\times\hat{\vec{B}}\right)\cdot\frac{\partial\hat{f}_a}{\partial\vec{v}}\right)\right\rangle_{ens}$

- Use **drift-ordering** to separate neoclassical and anomalous transport.

Sugama, PoP, vol. 5, 2560 (1998).

Expand in powers of ρ_* to derive the gyrokinetic, drift-kinetic, and transport equations.

Ensemble-averages:

$$f_a = f_{0a} + f_{1a} + f_{2a} + \ldots$$

$$\vec{E} = \vec{E}_{-1} + \vec{E}_0 + \vec{E}_1 + \vec{E}_2 + \ldots$$

$$\vec{B} = \vec{B}_0$$

$$S_a = S_{2a} + \ldots \quad \text{(transport ordering)}$$

Fluctuations:

$$\hat{f}_a = \hat{f}_{1a} + \hat{f}_{2a} + \ldots$$

$$\hat{\vec{E}} = \hat{\vec{E}}_1 + \hat{\vec{E}}_2 + \ldots$$

$$\hat{\vec{B}} = \hat{\vec{B}}_1 + \hat{\vec{B}}_2 + \ldots$$

- **Lowest order constraints:**

$$A_{-1} = 0: \quad \vec{E}_{-1} + \frac{1}{c}\vec{V}_0 \times \vec{B} = 0 \quad \text{and} \quad \frac{\partial f_{0a}}{\partial \xi} = 0$$

Large mean flow: $\vec{V}_0 = R\omega_0(\psi)\nabla\varphi$ where $\omega_0(\psi) = -c\frac{d\Phi_{-1}}{d\psi}$

- **Equilibrium equation:**

$$\oint \frac{d\xi}{2\pi} A_0 = 0: \quad \left(\vec{V}_0 + v_\parallel' \hat{b}\right)\cdot\nabla f_{0a} = C_{aa}\left(f_{0a}, f_{0a}\right) \quad \text{where} \quad \vec{v}'=\vec{v}-\vec{V}_0$$

$$\rightarrow f_{0a} = n_a(\psi,\theta)\left(\frac{m_a}{2\pi T_a}\right)^{3/2} e^{-m_a(v')^2/2T_a}$$

Maxwellian in the rotating frame

Gyroaverages of the O(ρ_*) ensemble-averaged and fluctuating equations give the drift-kinetic equation & gyrokinetic equation.

- **Drift-kinetic equation**:

$$\oint \frac{d\xi}{2\pi} A_1 = 0: \quad f_{1a} = \tilde{f}_{1a} + \overline{f}_{1a} \;, \quad \tilde{f}_{1a} = \frac{1}{\Omega_{ca}} \int^{\xi} d\xi \left(L f_{0a} \right)_{osc}$$

gyroangle -dependent

gyroangle -independent

  - **first-order (gyroangle-independent) ensemble-averaged distribution is determined by the DKE**

$$v_{\parallel}' \hat{b} \cdot \nabla \left(\overline{f}_{1a} - f_{0a} \frac{z_a e}{T_a} \Phi_1 \right) - C_a^L \left(\overline{f}_{1a} \right) = f_{0a} \left[-\frac{d \ln \left(N_a T_a \right)}{d\psi} W_{a1} - \frac{d \ln T_a}{d\psi} W_{a2} + \frac{c}{T_a} \frac{d^2 \Phi_{-1}}{d\psi^2} W_{aV} + \frac{\left\langle B E_{\parallel}^A \right\rangle}{T_a \left\langle B^2 \right\rangle^{1/2}} W_{aE} \right]$$

- **Gyrokinetic equation:**

$$\oint \frac{d\xi}{2\pi} F_1 = 0: \quad \hat{f}_{1a} \left(\vec{x} \right) = -\frac{z_a e}{T_a} \hat{\Phi}_1 + h_a \left(\vec{x} - \vec{\rho} \right)$$

  - **first-order fluctuating distribution in terms of the distribution of the gyrocenters, $h_a(R)$, is determined by the GKE**

$$\frac{\partial h_a \left(\vec{R} \right)}{\partial t} + \left(\vec{V}_0 + v_{\parallel}' \hat{b} + v_{da} - \frac{c}{B} \nabla \hat{\Psi}_a \times \hat{b} \right) \cdot \nabla h_a - C_a^{GL} \left(\hat{f}_{1a} \right) = f_{0a} \left[-\frac{\partial \ln \left(N_a T_a \right)}{\partial \psi} \hat{W}_{a1} - \frac{\partial \ln T_a}{\partial \psi} \hat{W}_{a2} + \frac{c}{T_a} \frac{\partial^2 \Phi_{-1}}{\partial \psi^2} \hat{W}_{aV} + \frac{1}{T_a} \hat{W}_{aT} \right]$$

Flux-surface-averaged moments of the FP equation to O(ρ_*^2) give the transport equations.

Density: $\left\langle \int d^3v A \right\rangle_\theta \rightarrow \frac{\partial \langle n_a \rangle}{\partial t} + \frac{1}{V'}\frac{\partial}{\partial r}\left(V'\Gamma_a\right) = S_{na}$

Energy: $\left\langle \int d^3v \varepsilon A \right\rangle_\theta \rightarrow \frac{3}{2}\frac{\partial \langle n_a T_a \rangle}{\partial t} + \frac{1}{V'}\frac{\partial}{\partial r}\left(V'Q_a\right) + \Pi_a \frac{\partial \omega_0}{\partial \psi} = S_{Wa}$

Toroidal momentum: $\left\langle \int d^3v m_a v'_\varphi A \right\rangle_\theta \rightarrow \frac{\partial}{\partial t}\left(\omega_0 \langle R^2 \rangle \sum_a m_a n_a\right) + \frac{1}{V'}\frac{\partial}{\partial r}\left(V' \sum_a \Pi_a\right) = \sum_a S_{\omega a}$

Particle flux: $\Gamma_a = \Gamma_a^{GV} + \Gamma_a^{neo} + \Gamma_a^{tur}$

Energy flux: $Q_a = Q_a^{GV} + Q_a^{neo} + Q_a^{tur}$

Momentum flux: $\Pi_a = \Pi_a^{GV} + \Pi_a^{neo} + \Pi_a^{tur}$

Outline

- Overview of kinetic theory
- **Drift-kinetic neoclassical simulations**
  - **Numerical algorithms**
  - Reduced models
- Integrated modeling
  - MHD equilibrium reconstruction
  - Steady-state transport
- Advanced physics effects
  - Strong toroidal rotation
  - Nonaxisymmetry
  - Nonlocal effects

Neoclassical codes solve the steady-state O(ρ_*) drift-kinetic-Poisson equations for the ensemble-averaged f.

- **Solve for $f_{1a}(r,\theta,\xi,x_a)$ and $\Phi_1(r,\theta)$** $\quad \xi=v_{||}/v,\ x_a=v/(2^{½}v_{ta})$

parallel streaming | trapping | collisions

$$\sqrt{2}v_{ta}x_a\xi\hat{b}\cdot\nabla f_{1a}+f_{0a}\frac{z_a e}{T_a}\sqrt{2}v_{ta}\xi\hat{b}\cdot\nabla\Phi_1-\frac{\sqrt{2}v_{ta}x_a}{2}\frac{\hat{b}\cdot\nabla B}{B}\left(1-\xi^2\right)\frac{\partial f_{1a}}{\partial\xi}-\sum_b C^L_{ab}\left(f_{1a},f_{1b}\right)$$

$$=-v_D\cdot\nabla f_{0a}-f_{0a}\frac{z_a e}{T_a}v_D\cdot\nabla\Phi_0 \quad \text{source}$$

$$0=\sum_a z_a e\int d^3v f_{1a} \quad \text{Poisson equation}$$

→ **Transport coefficients and flows**

$$\Gamma_a=\left\langle\int d^3v\left(f_{0a}\vec{v}_E^{(1)}\cdot\nabla r+f_{1a}\vec{v}_D\cdot\nabla r\right)\right\rangle\ ,\ Q_a=\left\langle\int d^3vT_{0a}x_a^2\left(f_{0a}\vec{v}_E^{(1)}\cdot\nabla r+f_{1a}\vec{v}_D\cdot\nabla r\right)\right\rangle\ ,\ u_{||}=\frac{1}{n_{0a}}\int d^3v\sqrt{2}v_{ta}x_a\xi f_{1a}$$

- **The Poisson eqn and the DKE can be uncoupled**

$$g_{1a}=f_{1a}+f_{0a}\frac{z_a e}{T_{0a}}\Phi_1$$ **Non-adiabatic distribution**

Not true if time-dependent: $\frac{\partial f_{1a}}{\partial t}\rightarrow\frac{\partial g_{1a}}{\partial t}-f_{0a}\frac{z_a e}{T_{0a}}\frac{\partial\Phi_1}{\partial t}$

$$\sum_b D_{ab}\left(g_{1a},g_{1b}\right)=R\left(f_{0a},\Phi_0\right)\ ,\ \sum_a\frac{n_{0a}z_a^2e^2}{T_{0a}}\Phi_1=\sum_a z_a e\int d^3v g_{1a}\Rightarrow\Gamma_{2a}=\left\langle\int d^3v g_{1a}\vec{v}_D\cdot\nabla r\right\rangle$$

Fluid approach

- e.g. NCLASS, NEOART
- Assume **distribution function truncation** (13M)

$$f_{1a} = f_{0a}\frac{2\vec{v}}{v_{ta}^2}\cdot\left[\vec{u}_a + \frac{2}{5}\frac{\vec{q}_i}{p_i}\left(\frac{v^2}{v_{ti}^2} - \frac{5}{2}\right)\right]$$

- **Parallel momentum balance eqns**

Viscous stress tensors **friction forces**

$$\left\langle \vec{B}\cdot\nabla\cdot\vec{\vec{\Pi}}_a \right\rangle = \left\langle \vec{B}\cdot\vec{F}_{1a} \right\rangle \;,\; \left\langle \vec{B}\cdot\nabla\cdot\vec{\vec{\Theta}}_a \right\rangle = \left\langle B\cdot\vec{F}_{2a} \right\rangle \qquad \vec{F}_{ja} = \int d^3v m_a \vec{v} L_{j-1}^{3/2}\left(v^2/v_{ta}^2\right)\sum_b C_{ab}^L\left(f_{1a}, f_{1b}\right)$$

- Using f_{1a}, relate to poloidal and parallel flows

viscosity coeffs

$$\left\langle \vec{B}\cdot\nabla\cdot\vec{\vec{\Pi}}_a \right\rangle = n_{0a}m_a\tau_{aa}^{-1}\left\langle B^2\right\rangle\left(\hat{\mu}_{1a}\hat{u}_{\theta a} + \hat{\mu}_{2a}\hat{q}_{\theta a}\right) \;,\; \left\langle \vec{B}\cdot\nabla\cdot\vec{\vec{\Theta}}_a \right\rangle = n_{0a}m_a\tau_{aa}^{-1}\left\langle B^2\right\rangle\left(\hat{\mu}_{2a}\hat{u}_{\theta a} + \hat{\mu}_{3a}\hat{q}_{\theta a}\right)$$

$$\left\langle \vec{B}\cdot\vec{F}_{1a} \right\rangle = n_{0a}m_a\tau_{aa}^{-1}\sum_b\left(\hat{l}_{11,ab}\left\langle u_{\parallel,a}B\right\rangle - \hat{l}_{12,ab}\left\langle q_{\parallel,a}B\right\rangle\right) \;,\; \left\langle \vec{B}\cdot\vec{F}_{2a} \right\rangle = n_{0a}m_a\tau_{aa}^{-1}\sum_b\left(\hat{l}_{21,ab}\left\langle u_{\parallel,a}B\right\rangle - \hat{l}_{22,ab}\left\langle q_{\parallel,a}B\right\rangle\right)$$

friction coeffs

- **Radial momentum balance eqns**

$$\vec{u}_{\perp,a} = \left(\vec{B}/B^2\right)\times\left[\nabla p_{0a}/(z_a n_{0a}e) + \nabla\Phi\right] \;,\; \vec{\mathrm{q}}_{\perp,a} = \left(\vec{B}/B^2\right)\times\nabla T_{0a}/(z_a n_{0a}e)$$

Fluid approach (continued)

- Use **incompressibility** eqns to relate parallel and poloidal flows

$$\nabla\cdot\left(n_{0a}\vec{u}_a\right)=0\ ,\ \nabla\cdot\vec{q}_a=0$$

$$u_{\|,a}=V_{1a}+\hat{u}_{\theta a}(\psi)B\ ,\ u_{\theta a}=\hat{u}_{\theta a}(\psi)B_\theta\ ,\ V_{1a}=-T_{0a}/\left(z_aB_\theta\right)\left(d\ln p_{0a}/dr+z_a/T_{0a}d\Phi/dr\right)$$

$$q_{\|,a}=V_{2a}+\hat{q}_{\theta a}(\psi)B\ ,\ \mathrm{q}_{\theta a}=\hat{q}_{\theta a}(\psi)B_\theta\ ,\ V_{2a}=-1/\left(z_aB_\theta\right)dT_{0a}/dr$$

- Final set of eqns for poloidal flows
  - **Only 2*$n_{species}$ linear algebraic eqns**

$$\sum_b\left[\begin{pmatrix}\hat{\mu}_{1a}&\hat{\mu}_{2a}\\ \hat{\mu}_{2a}&\hat{\mu}_{3a}\end{pmatrix}\delta_{ab}-\begin{pmatrix}\hat{l}_{11,ab}&-\hat{l}_{12,ab}\\ -\hat{l}_{12,ab}&\hat{l}_{22,ab}\end{pmatrix}\right]\begin{pmatrix}\hat{u}_{\theta b}\\ \hat{q}_{\theta b}\end{pmatrix}=\sum_b\begin{pmatrix}\hat{l}_{11,ab}&-\hat{l}_{12,ab}\\ -\hat{l}_{12,ab}&\hat{l}_{22,ab}\end{pmatrix}\begin{pmatrix}\langle V_{1b}B\rangle/\langle B^2\rangle\\ \langle V_{2b}B\rangle/\langle B^2\rangle\end{pmatrix}$$

$$\Gamma_a=\Gamma_a^{BP}+\Gamma_a^{PS}\ ,\ \mathrm{Q}_a=Q_a^{BP}+Q_a^{PS}$$ → **Transport coefficients and flows**

$$\{\Gamma,Q\}_a^{BP}=\frac{-I}{\psi' z_a e\langle B^2\rangle}\left\langle\vec{B}\cdot\left\{\vec{F}_{1a},T_{0a}\vec{F}_{2a}\right\}\right\rangle\ ,\ \{\Gamma,Q\}_a^{PS}=\frac{-I}{\psi' z_a e}\left\langle\vec{B}\cdot\left\{\vec{F}_{1a},T_{0a}\vec{F}_{2a}\right\}\left(\frac{1}{B^2}-\frac{1}{\langle B^2\rangle}\right)\right\rangle$$

- **But need analytic approximations for viscosity coeffs**

Kinetic approach

- **DKE is solved for the full form of f and then the transport coefficients are computed directly from f**
  - $n_{species}*n_{energy}*n_{pitchangle}*n_{theta}$
- No approximations beyond the drift ordering
- Essential effects needed: general geometry, accurate collision models, multi-species
- Numerical method
  - **PIC**: GTC-NEO, XGC0, FORTEC
  - **Eulerian**: CQLP, PERFECT, NEO

The ambipolarity property requires complete cross-species collisional coupling.

Operate on the kinetic equation with $\langle \int d^3v (v_{||}/B) \ldots \rangle$:

$$\Gamma_{2a} = -\left\langle \frac{I}{\psi' \Omega_a} \int d^3v v_{||} \sum_b C_{ab} g_{1b} \right\rangle$$

$$\Downarrow$$

$$\sum_a Z_a \Gamma_{2a} = -c \left\langle \frac{I}{\psi' eB} \int d^3v \sum_{a,b} m_a v_{||} C_{ab} g_{1b} \right\rangle$$

The plasma maintains ambipolarity only if the momentum conservation properties of C_{ab} are properly maintained.

In practice, C_{ie} is often neglected (but not in NEO). This has implications for transport in the deep PS regime.

With the full linearized Fokker-Planck collision operator, codes can give the exact solution for the local neoclassical transport.

- **Test particle component**
  - Lorentz + Diffusion

$$C^{T}_{ab}\left(f_{1a},f_{0b}\right)=\frac{\nu^{D}_{ab}(v)}{2}\frac{\partial}{\partial\xi}\left(1-\xi^{2}\right)\frac{\partial f_{1a}}{\partial\xi}+\frac{1}{2v^{2}}\frac{\partial}{\partial v}\left[\nu^{\|}_{ab}(v)\left(v^{4}\frac{\partial f_{1a}}{\partial v}+\frac{m_a}{T_{0b}}v^{5}f_{1a}\right)\right]$$

- **Field particle component**

$$\xi = v_{\|}/v$$

  - Momentum and energy conserving

$$C^{F}_{ab}\left(f_{0a},f_{1b}\right)/\Gamma_a=-\frac{1}{v^{2}}\frac{\partial}{\partial v}\left(f_{0a}v^{2}\frac{\partial H_b}{\partial v}\right)-f_{0a}\frac{1}{v^{2}}\frac{\partial}{\partial\xi}\left[\left(1-\xi^{2}\right)\frac{\partial H_b}{\partial\xi}\right]+\frac{1}{2v^{2}}\frac{\partial^{2}}{\partial v^{2}}\left[f_{0a}v^{2}\frac{\partial^{2}G_b}{\partial v^{2}}\right]$$

$$+f_{0a}\frac{1}{2v^{2}}\frac{\partial^{2}}{\partial\xi^{2}}\left[\frac{1}{v^{2}}\left(1-\xi^{2}\right)^{2}\frac{\partial^{2}G_b}{\partial\xi^{2}}+\frac{1}{v}\left(1-\xi^{2}\right)\frac{\partial G_b}{\partial v}-\frac{\xi}{v^{2}}\left(1-\xi^{2}\right)\frac{\partial G_b}{\partial\xi}\right]$$

$$+\frac{1}{v^{2}}\frac{\partial^{2}}{\partial\xi\partial v}\left\{f_{0a}\left(1-\xi^{2}\right)\left[\frac{\partial^{2}G_b}{\partial\xi\partial v}-\frac{1}{v}\frac{\partial G_b}{\partial\xi}\right]\right\}+\frac{1}{2v^{2}}\frac{\partial}{\partial v}\left\{f_{0a}\left[-\frac{1}{v}\left(1-\xi^{2}\right)\frac{\partial^{2}G_b}{\partial\xi^{2}}-2\frac{\partial G_b}{\partial v}+\frac{2\xi}{v}\frac{\partial G_b}{\partial\xi}\right]\right\}$$

$$+f_{0a}\frac{1}{2v^{2}}\frac{\partial}{\partial\xi}\left[\frac{\xi}{v^{2}}\left(1-\xi^{2}\right)\frac{\partial^{2}G_b}{\partial\xi^{2}}+\frac{2\xi}{v}\frac{\partial G_b}{\partial v}+\frac{2}{v}\left(1-\xi^{2}\right)\frac{\partial^{2}G_b}{\partial\xi\partial v}-\frac{2}{v^{2}}\frac{\partial G_b}{\partial\xi}\right]$$

$$\Gamma_a=\frac{4\pi z_a^{4}e^{4}}{m_a^{2}}$$

Rosenbluth potentials:

$$H_b=\left(1+\frac{m_a}{m_b}\right)\frac{z_b^{2}}{z_a^{2}}\ln\Lambda_{ab}h_b,\; G_b=\frac{z_b^{2}}{z_a^{2}}\ln\Lambda_{ab}g_b$$

$$\nabla^{2}_{v}h_b=-4\pi f_{1b}\quad,\nabla^{2}_{v}g_b=2h_b$$

The velocity-space coordinates are chosen for optimal accuracy of the collision dynamics.

Gyrokinetic codes are optimized for the collisionless problem.

e.g. GYRO, GS2 use (ε,λ) coordinates

$$\lambda = \mu / \varepsilon$$

- Direct treatment of particle bounce points

$$v_{\parallel}(\theta) = \sigma\sqrt{2\varepsilon\left[1-\lambda B(\theta)\right]}$$

$$\sigma = \mathrm{sgn}(v_{\parallel})$$

- No continuity of f(λ) is assumed across the TP boundary at $\lambda_{TP}=1/B(\pi)$
- Gyroaverage op is 1D
- Maps to irregular grid in (ξ,θ)

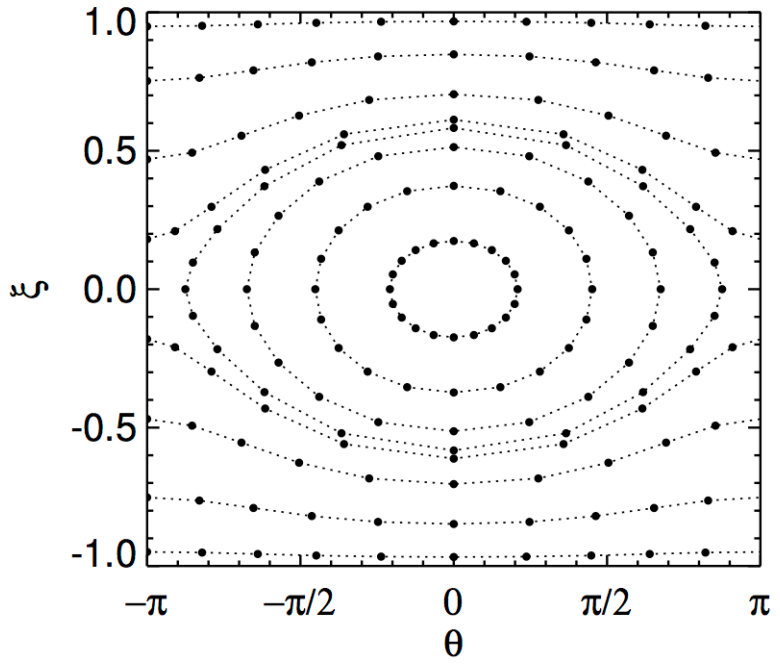

Neoclassical codes require more accurate treatment of collisions.

$$\xi = v_{\parallel} / v$$

$$x_a = v / \left(\sqrt{2} v_{ta}\right)$$

Legendre Polynomials in Cosine of Pitch Angle

$$g_{1a} = f_{0a} \sum_{l=0}^{N_\xi} \hat{g}_{1a}^{l}(\theta, x_a) P_l(\xi)$$

velocity coords: $\xi = v_\parallel / v$, $x_a = v / \left(\sqrt{2} v_{ta}\right)$

- **Collocation integrals can be done analytically** $\frac{2l+1}{2} \int_{-1}^{1} d\xi P_l(\xi)$
- **Matrix is sparse in this dimension**
  - Collisionless components are tri-diagonal
  - Collisional components are diagonal
- **Transport coefficients are simplified**

$$\{\Gamma_a, Q_a\} = \frac{4 n_{0a}}{\sqrt{\pi}} \left\langle \left(-\rho_a v_{ta} \frac{I}{\psi'} \frac{\hat{b} \cdot \nabla B}{B} \right) \int_0^\infty dx_a e^{-x_a^2} \left\{ x_a^4, T_{0a} x_a^6 \right\} \hat{g}_{1a}^{l} \left(\frac{4}{3} \delta_{l,0} + \frac{2}{3} \delta_{l,2} \right) \right\rangle$$

$$u_{\parallel,a} = \frac{8 v_{ta}}{3\sqrt{2\pi}} \int_0^\infty dx_a e^{-x_a^2} x_a^3 \hat{g}_{1a}^{l} \delta_{l,1}$$

- **Disadvantage: Need large number of modes at low collisionality**

The numerical issue is that f is discontinuous at the trapped/ passing boundary for the collisionless solution.

$$\sqrt{2}v_{ta}x_a\xi\hat{b}\cdot\nabla g_{1a} - \frac{\sqrt{2}v_{ta}x_a}{2}\frac{\hat{b}\cdot\nabla B}{B}\left(1-\xi^2\right)\frac{\partial g_{1a}}{\partial\xi} - \sum_b C^L_{ab}\left(g_{1a},g_{1b}\right) = -v_D\cdot\nabla f_{0a} - f_{0a}\frac{z_a e}{T_a}v_D\cdot\nabla\Phi_0$$

- The streaming+trapping terms have the form: $\dot{\theta}\frac{\partial}{\partial\theta}+\dot{\xi}\frac{\partial}{\partial\xi}$ $\qquad \dot{\theta}=\frac{v}{L_\parallel}\xi\ ,\ \dot{\xi}=\frac{v}{L_\parallel}\left(\frac{1-\xi^2}{2}\right)\varepsilon\sin\theta$

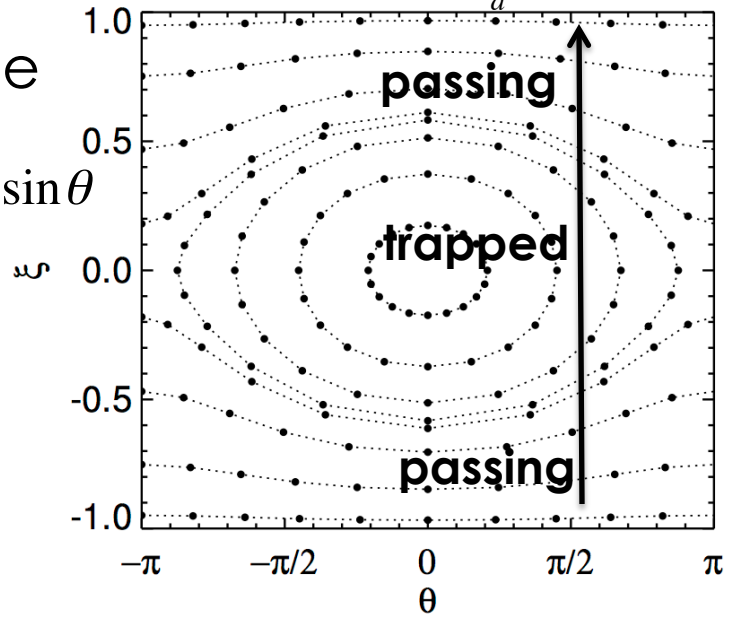

- This can be written as:

$$\ddot{\theta}=\left(\frac{v}{L_\parallel}\right)^2\left[\frac{1-\dot{\theta}^2\left(L_\parallel/v\right)^2}{2}\right]\varepsilon\sin\theta$$

- Treating ε as a small parameter, the characteristics of the streaming+trapping terms have the associated integral of motion: $\dot{\theta}^2=\dot{\theta}_0^2+\left(1-\dot{\theta}_0^2\right)\varepsilon\cos\theta$
- **Without collisions, there is no mechanism to ensure that g is continuous between passing and trapped particles → low collisionality may be very inefficient.**

(ξ, θ) contour plots
Remnants of the t/p boundary disappear as ν increases.

ion

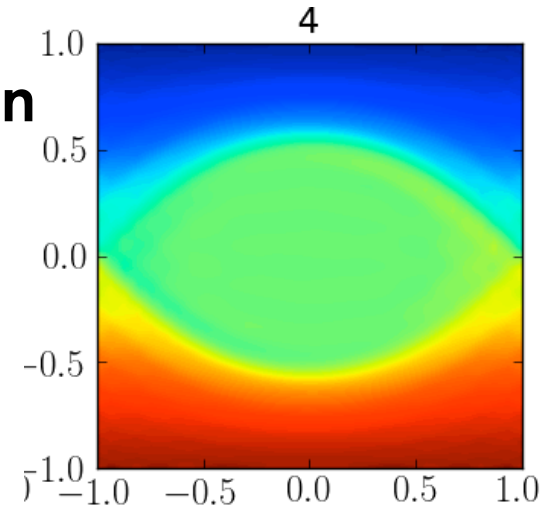

ν_{*e}=0.005

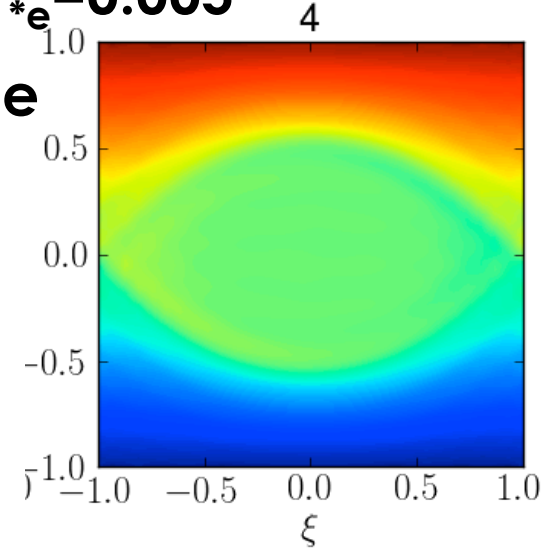

ele

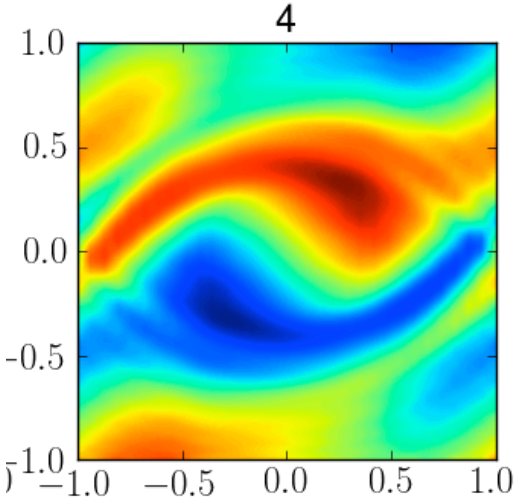

ν_{*e}=0.5

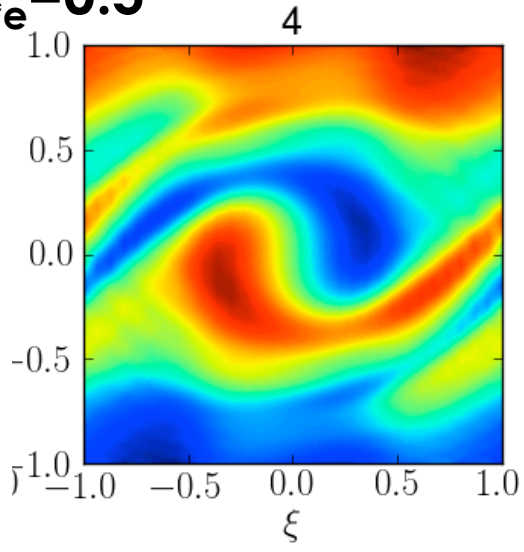

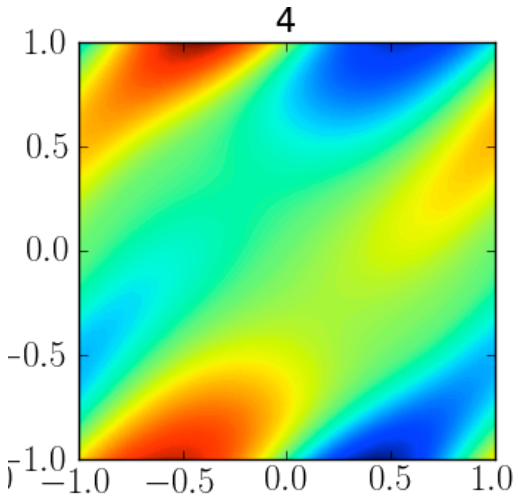

ν_{*e}=50

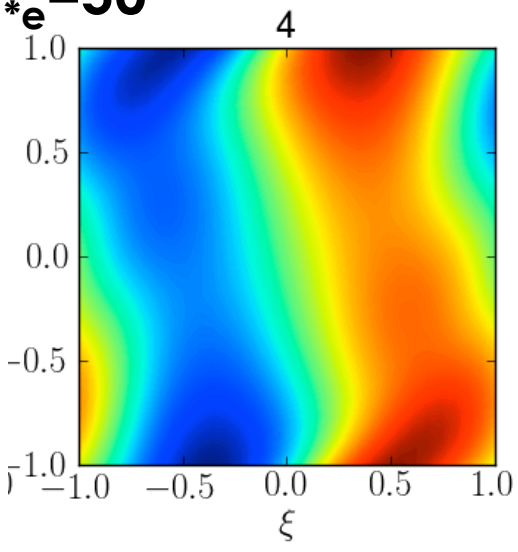

Laguerre polynomials in energy

$$g_{1a} = f_{0a} \sum_{l=0}^{N_\xi} \sum_{m=0}^{N_x} \hat{g}_{1a}^{lm}(\theta) P_l(\xi) L_m^{k(l)+1/2}\left(x_a^2\right) x_a^{k(l)}$$

Laguerre-(1/2+3/2)

$$\{k(l)=0, l=0;\ k(l)=1, l>0\}$$

- **Can accurately compute energy derivative, integration on infinite domain, and apparent singularities in the collision frequency**

$$C_{ab}^T\left(g_{1a}, f_{0b}\right) = \frac{\nu_{ab}^D}{2} \frac{\partial}{\partial \xi}\left(1-\xi^2\right)\frac{\partial g_{1a}}{\partial \xi} + \frac{1}{2v^2}\frac{\partial}{\partial v}\left[\nu_{ab}^{\parallel}\left(v^4 \frac{\partial g_{1a}}{\partial v} + \frac{m_a}{T_{0b}} v^5 g_{1a}\right)\right]$$

$$\nu_{ab}^D(v) = \tau_{ab}^{-1} x_a^{-3}\left[\frac{1}{\sqrt{\pi} x_b} e^{-x_b^2} + erf\left(x_b\right)\left(1-\frac{1}{2x_b^2}\right)\right] \quad , \quad \nu_{ab}^{\parallel}(v) = 2\tau_{ab}^{-1} x_a^{-3}\left[\frac{1}{\sqrt{\pi} x_b} e^{-x_b^2} + erf\left(x_b\right)\left(\frac{1}{2x_b^2}\right)\right]$$

- **Collocation integrals can be written in terms of Gamma functions (collisionless)**

$$\frac{2l+1}{2}\int_{-1}^{1} d\xi P_l(\xi) \int_0^{\infty} dx_a L_m^{k(l)+1/2}\left(x_a^2\right) x_a^{k(1)+2}$$

- **Disadvantage: Matrix is dense in this dimension**

Laguerre basis collocation integrals are determined from analytic expressions in the monomial basis.

Mapping between Laguerre and monomial basis:

$$L_m^{k(l)+1/2}\left(x_a^2\right) = \sum_{j=0}^{m} \Lambda_{mj}^k x^{2j}$$

$$\Lambda_{mj}^k = \frac{(-1)^j}{j!}\begin{pmatrix} m+k+1/2 \\ m-j \end{pmatrix}$$

Discrete forms of the collision operator can be written in terms of 2 functions:

$$F(\lambda_{aa'},m,n) = \int_0^\infty dx e^{-x^2} x^m \int_0^x dy e^{-\lambda_{aa'}y^2} y^n$$

$$\bar{F}(\lambda_{aa'},m,n) = \int_0^\infty dx e^{-x^2} x^m \int_x^\infty dy e^{-\lambda_{aa'}y^2} y^n$$

$$\lambda_{a,a'} = v_{ta}^2 / v_{ta'}^2$$

Accurate numerical evaluation of the collision integrals is non-trivial, but can be determined by a series of gamma & beta funcs.

$$F(\lambda,m,n)=\int_0^\infty dx e^{-x^2}x^m\int_0^x dy e^{-\lambda y^2}y^n \quad\Rightarrow\quad F(\lambda,m,n)=\frac{1}{4\lambda^{(n+1)/2}}\int_0^\infty dt e^{-t}t^{(m-1)/2}\gamma\left(\frac{n+1}{2},\lambda t\right)$$

$$\bar{F}(\lambda,m,n)=\int_0^\infty dx e^{-x^2}x^m\int_x^\infty dy e^{-\lambda y^2}y^n \quad\Rightarrow\quad \bar{F}(\lambda,m,n)=\frac{1}{4\lambda^{(n+1)/2}}\int_0^\infty dt e^{-t}t^{(m-1)/2}\Gamma\left(\frac{n+1}{2},\lambda t\right)$$

$$\lambda_{a,a'}=v_{ta}^2/v_{ta'}^2$$

Develop a recursive method:

$$\{\gamma,\Gamma\}(s,x)=(s-1)\{\gamma,\Gamma\}(s-1,x)-x^{s-1}e^{-x}$$

⇒ e.g. (m,n)=(even,odd)

$$\bar{F}(\lambda,m,n)=\frac{\Gamma^2\left(\frac{n+1}{2}\right)\Gamma\left(\frac{m+1}{2}\right)}{4\lambda^{(n+1)/2}\Gamma\left(1+\frac{m+n}{2}\right)}\sum_{i=0}^{(n-1)/2}\frac{\lambda^i}{(1+\lambda)^{i+(m+1)/2}}\frac{\Gamma\left(i+\frac{m+1}{2}\right)}{\Gamma(i+1)}$$

Use reflection and sum identities:

$$F(\lambda_{aa'},m,n)=\bar{F}(1/\lambda_{aa'},m,n)$$

$$F(\lambda_{aa'},m,n)+\bar{F}(\lambda_{aa'},m,n)=B\left(\frac{m+1}{2},\frac{n+1}{2}\right)\Gamma\left(\frac{m+n}{2}+1\right)\frac{1}{4\lambda_{aa'}^{(n+1)/2}}$$

The distribution functions are computed via direct matrix solve.

$$\sum_{j=0}^{m}\sum_{j'=0}^{m'}\Lambda_{mj}^{k}\Lambda_{m'j'}^{k'}A_{aa'}^{ll',jj',ii'}\hat{g}_{1a'}^{l'm'i'}=-\sum_{j=0}^{m}\Lambda_{mj}^{k}S_{a}^{lji}$$

- **NEO solves an NxN matrix problem, where $N=N_s N_\xi N_x N_\theta$**
- A and S are the matrix elements and source in the monomial energy basis

$$A_{aa'}^{ll',jj'}(\theta)=\frac{\nu_{ta}}{\sqrt{2}J_\psi B}\delta_{aa'}\Gamma\left(j+j'+\frac{k(l)+k(l')}{2}+2\right)\left[\begin{array}{l}\left(\frac{l+1}{2l+3}\delta_{(l+1)l'}+\frac{l}{2l-1}\delta_{(l-1)l'}\right)\frac{\partial}{\partial\theta}\\ -\frac{1}{2}\frac{\partial\ln B}{\partial\theta}\left(\frac{(l+1)(l+2)}{2l+3}\delta_{(l+1)l'}-\frac{l(l-1)}{2l-1}\delta_{(l-1)l'}\right)\end{array}\right]-\left(C^T\right)_{aa'}^{ll',jj'}-\left(C^F\right)_{aa'}^{ll',jj'}$$

$$S_a^{lj}(\theta)=W_{0a}(\theta)\left(\frac{1}{2L_{1a}}\Gamma\left(j+k(0)/2+5/2\right)+\frac{1}{2L_{2a}}\Gamma\left(j+k(0)/2+7/2\right)\right)\left(\frac{4}{3}\delta_{l0}+\frac{2}{3}\delta_{l2}\right)$$

- The LHS matrix is
  - Tri-diagonal in ξ (l)
  - Dense in energy (m)
  - Penta-diagonal in theta (i)
  - Dense in species (a)

Numerical convergence properties

$$g_{1a} = f_{0a} \sum_{l=0}^{N_\xi} \sum_{m=0}^{N_x} \hat{g}_{1a}^{lm}(\theta) P_l(\xi) L_m^{k(l)+1/2}\left(x_a^2\right) x_a^{k(l)} \qquad \{k(l)=0, l=0;\ k(l)=1, l>0\}$$

adiabatic electrons

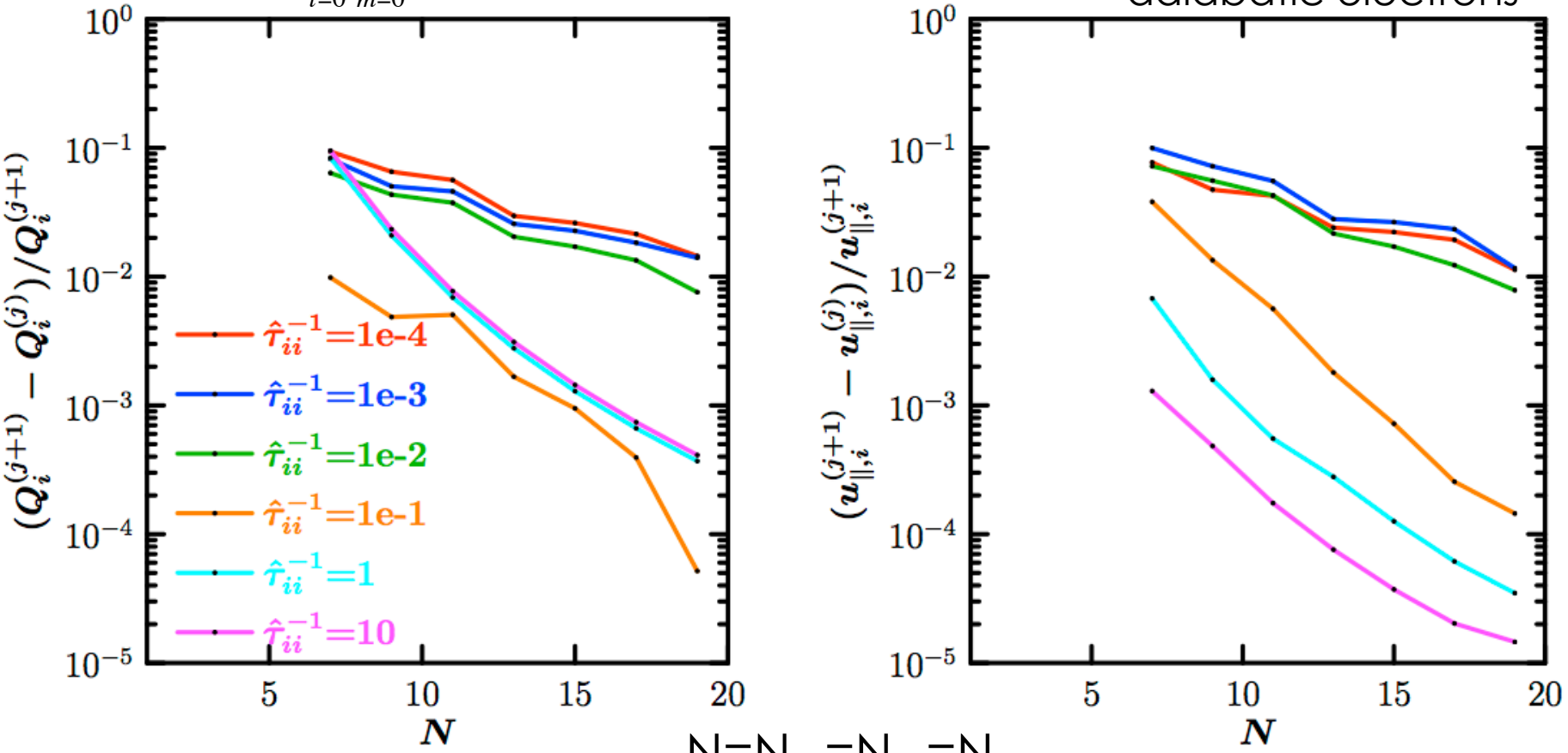

$N=N_\theta=N_\xi=N_x$

GA standard case: s-α geo, r/a=0.5, q=2, a/L_T=3, a/L_n=1, $T_{0i}=T_{0e}$

The method works well even with kinetic electrons.

$$g_{1a} = f_{0a} \sum_{l=0}^{N_\xi} \sum_{m=0}^{N_x} \hat{g}_{1a}^{lm}(\theta) P_l(\xi) L_m^{k(l)+1/2}\left(x_a^2\right) x_a^{k(l)} \qquad \{k(l)=0, l=0;\ k(l)=1, l>0\}$$

kinetic electrons

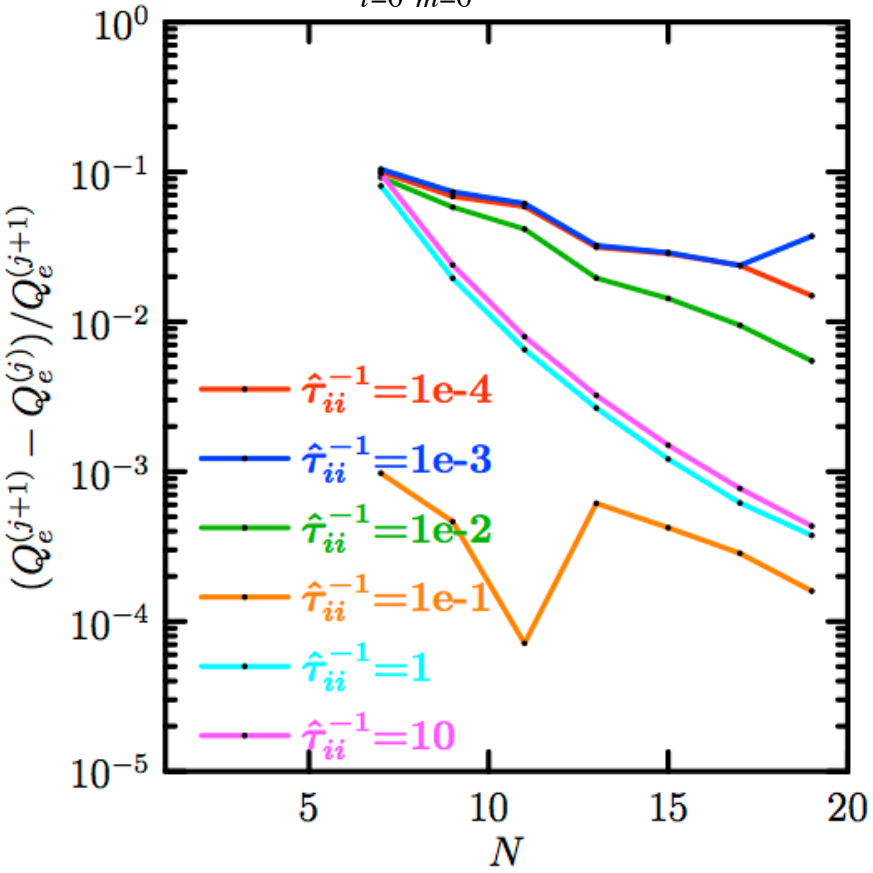

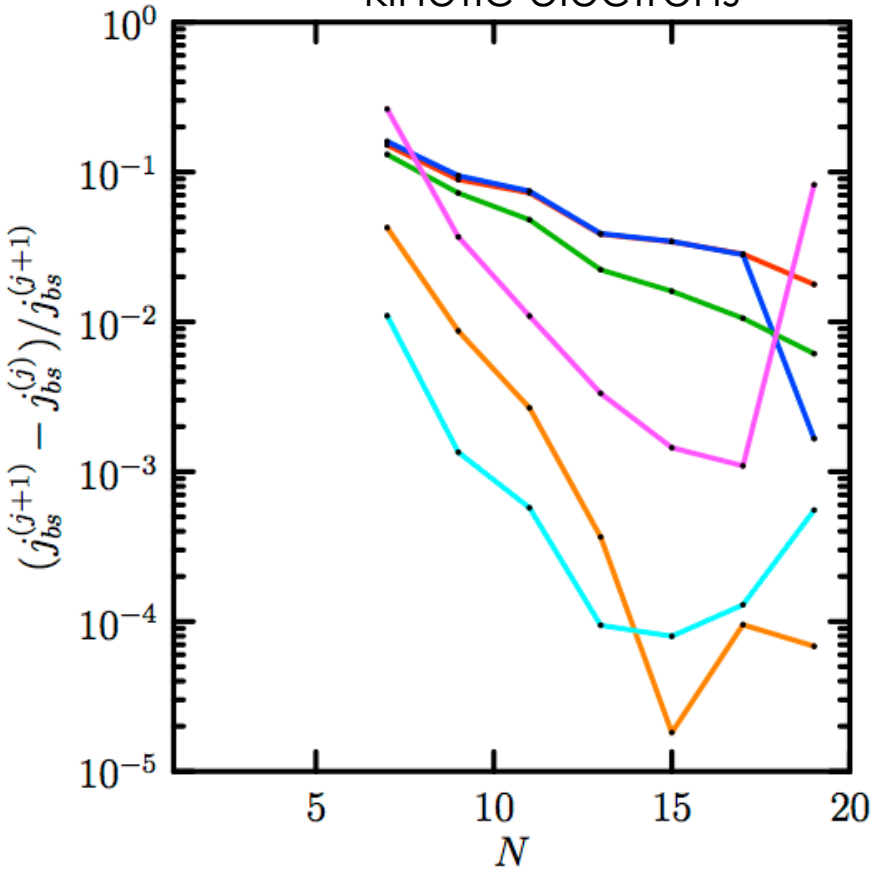

Even with multiple species, ambipolarity is maintained to a high degree of accuracy.

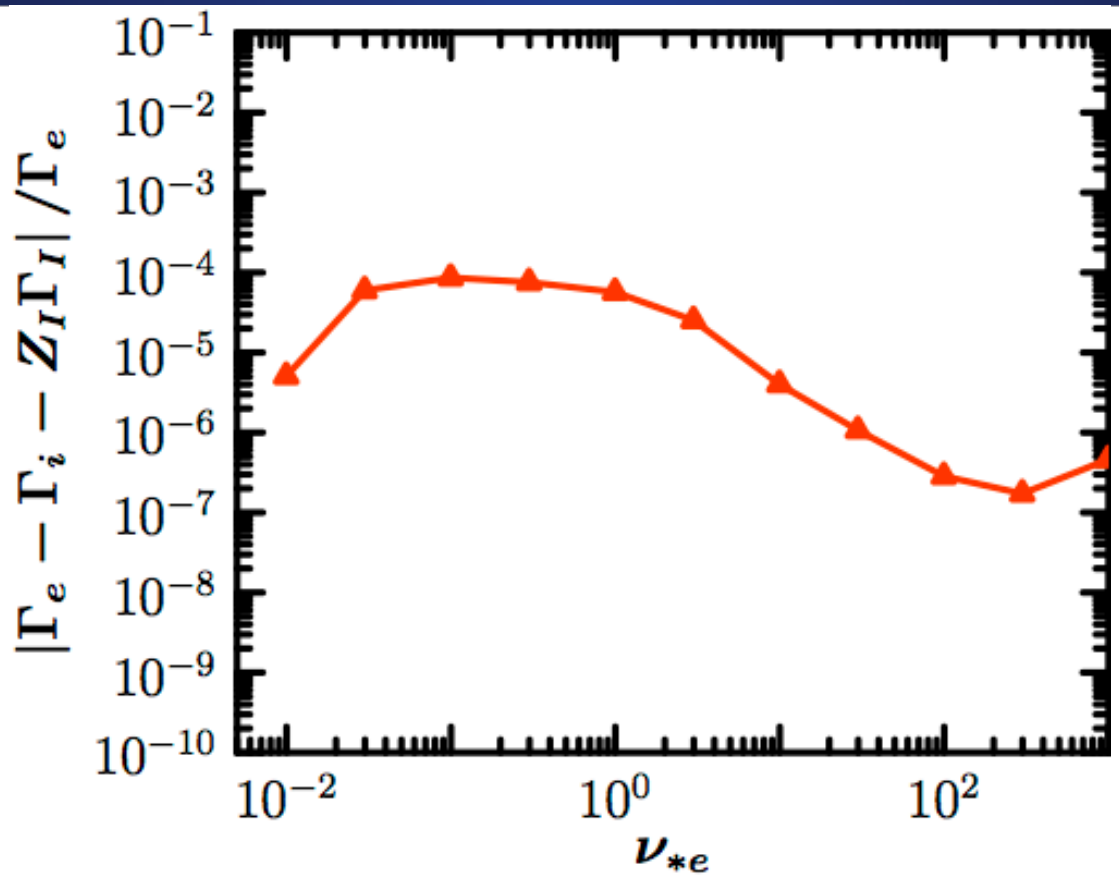

GA standard case + Carbon impurity:
$f_I = Z_I(n_{0I}/n_{0e}) = 0.1$

The Sonine method is subject to rapid numerical precision loss at large N due to high powers of energy.

Sonine: $$g_{1a} = f_{0a} \sum_{l=0}^{N_\xi} \sum_{m=0}^{N_x} \hat{g}_{1a}^{lm}(\theta) P_l(\xi) L_m^{k(l)+1/2}\left(x_a^2\right) x_a^{k(l)} \quad k(l) = l$$

adiabatic electrons

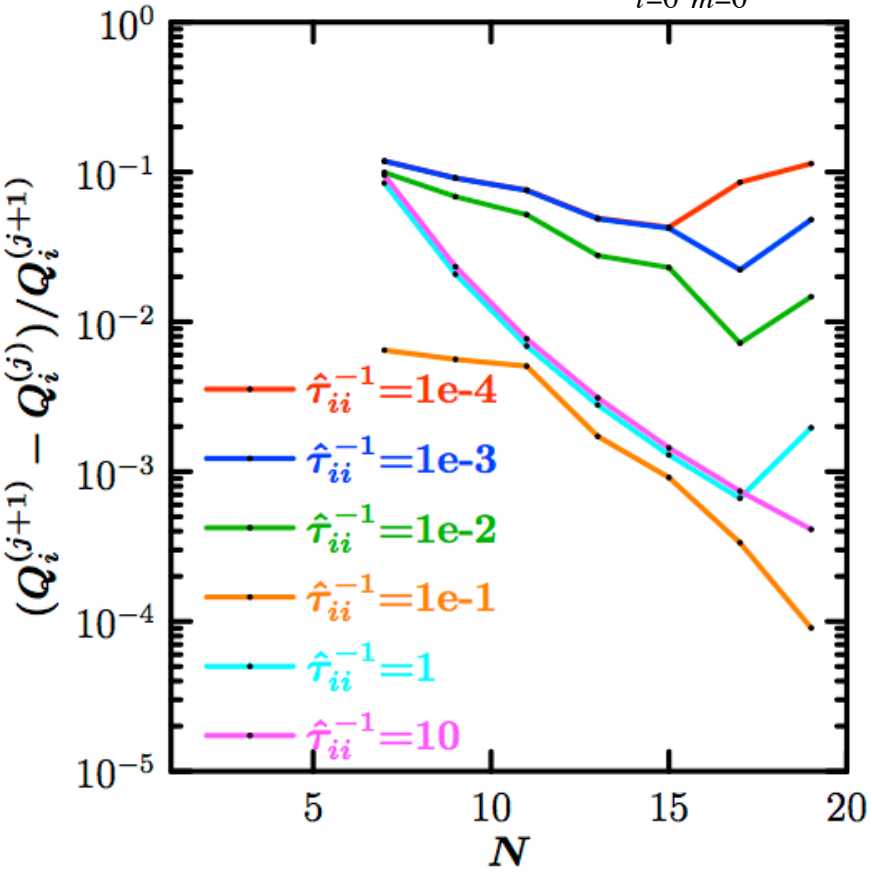

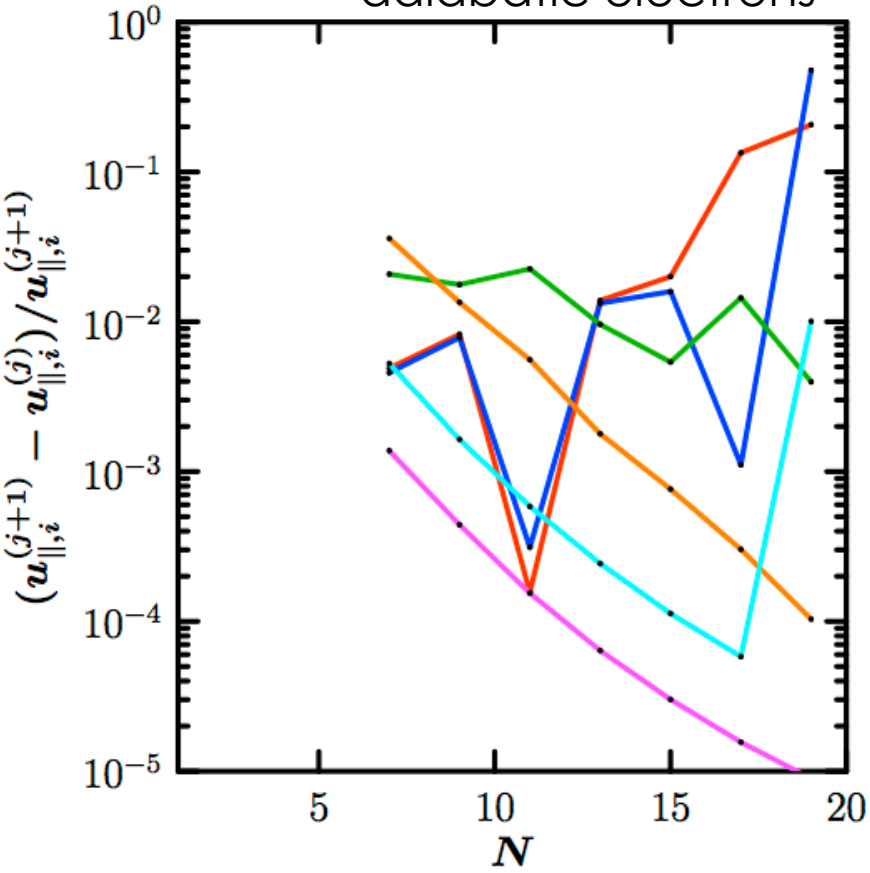

For experimental analysis, NEO is run in subroutine mode with variable theta resolution, trivially parallelized in radius.

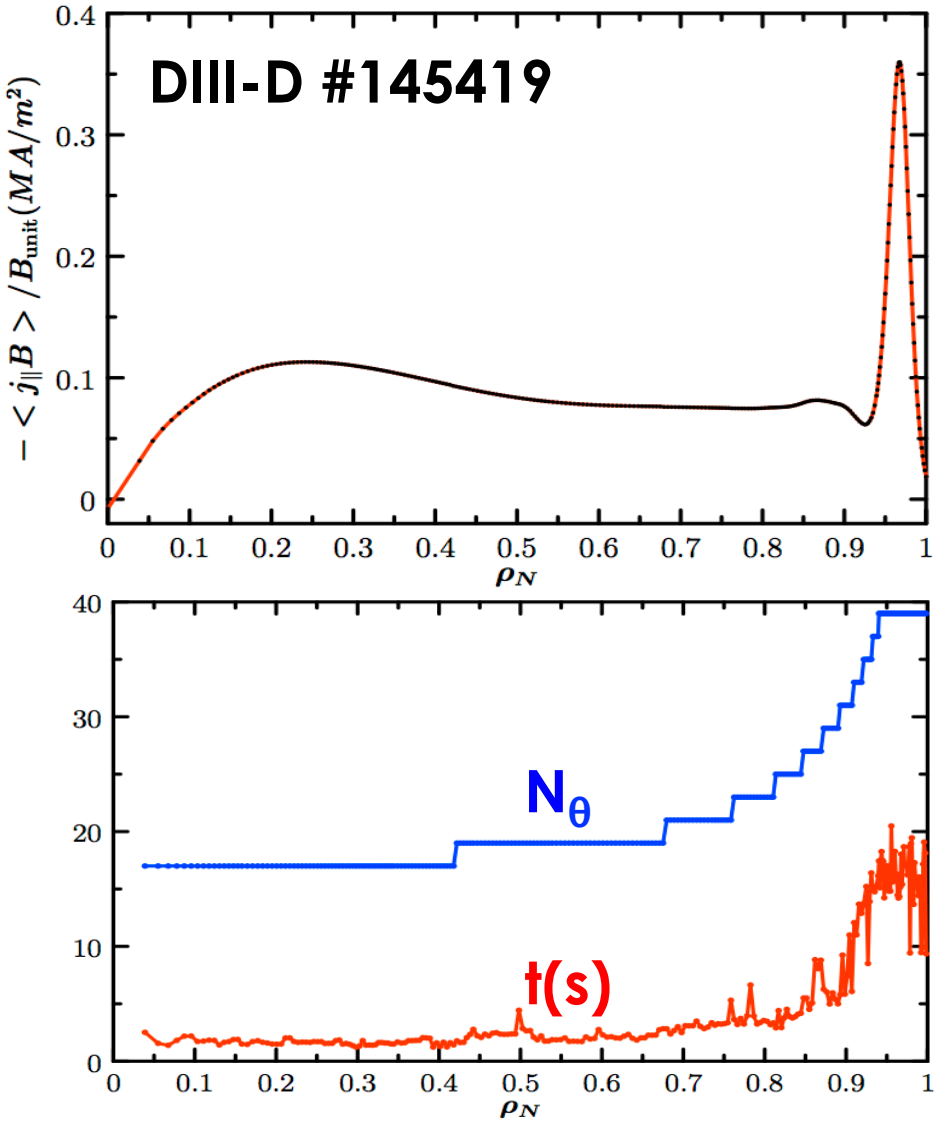

N_s=3
N_x=6
N_ξ=17

N_r=256
25min
0.5-2GB/r_i

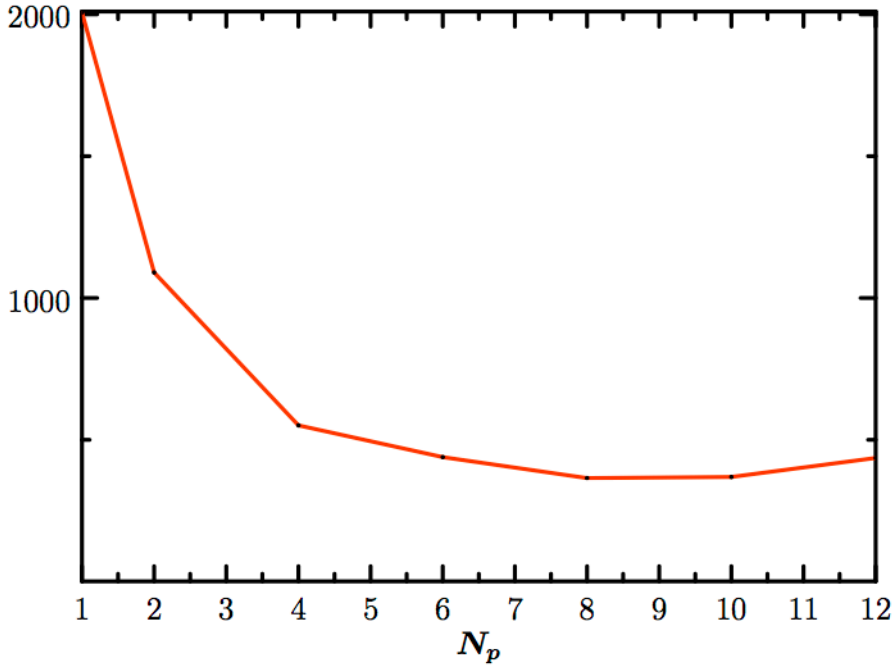

Outline

- **Overview of kinetic theory**
- **Drift-kinetic neoclassical simulations**
  - Numerical algorithms
  - **Reduced models**
- **Integrated modeling**
  - MHD equilibrium reconstruction
  - Steady-state transport
- **Advanced physics effects**
  - Strong toroidal rotation
  - Nonaxisymmetry
  - Nonlocal effects

Due to the complexity of the linearized FP operator, most neoclassical codes use reduced collision models.

- **Connor**

$$C^L_{ab}\left(f_{1a},f_{1b}\right)=\nu_{ab}Lf_{1a}+\mathrm{v}_{\|}\left(\nu_{ab}\frac{r_{ba}}{\mathrm{v}^2_{ta}}\right)f_{0a}$$

$$\begin{aligned}\nu_{ab}&=\nu^D_{ab},m_a=m_b\\&=\left(v/\sqrt{2}v_{ta}\right)^{-3}\tau^{-1}_{ab}\ ,m_a<<m_b\\&=\left(4/3\sqrt{\pi}\right)\sqrt{m_b/m_a}\left(T_{0a}/T_{0b}\right)^{3/2}\tau^{-1}_{ab}\ ,m_b<<m_a\end{aligned}$$

- **Zeroth-Order Hirshman-Sigmar**

$$C^L_{ab}\left(f_{1a},f_{1b}\right)=\nu^D_{ab}Lf_{1a}+\mathrm{v}_{\|}\left[\nu^s_{ab}\frac{r_{ba}}{\mathrm{v}^2_{ta}}+\left(\nu^D_{ab}-\nu^s_{ab}\right)\frac{u_a}{\mathrm{v}^2}\right]f_{0a}$$

$$\nu^D_{ab}=H\left(v/\sqrt{2}v_{tb}\right)\left(v/\sqrt{2}v_{ta}\right)^{-3}\tau^{-1}_{ab}$$

$$\nu^s_{ab}=G\left(v/\sqrt{2}v_{tb}\right)\left(v/\sqrt{2}v_{ta}\right)^{-1}\left(2T_{0a}/T_{0b}\right)\left(1+m_b/m_a\right)\tau^{-1}_{ab}$$

- **Test particle with ad hoc field particle (i-e approx)**

$$C^F_{ab}\left(f_{0a},f_{1b}\right)=-\frac{m_b}{m_a}C^T_{ab}\left(v_{\|}f_{0a},f_{0b}\right)\frac{\int d^3vv_{\|}C^T_{ba}\left(f_{1b},f_{0a}\right)}{\int d^3vv_{\|}C^T_{ab}\left(v_{\|}f_{0a},f_{0b}\right)}$$

$$-\frac{m_b}{m_a}C^T_{ab}\left(v^2f_{0a},f_{0b}\right)\frac{\int d^3vv^2C^T_{ba}\left(f_{1b},f_{0a}\right)}{\int d^3vv^2C^T_{ab}\left(v^2f_{0a},f_{0b}\right)}$$

$$C_{ie}=0,$$

$$C_{ei}=C_{ei,Connor}$$

The model operators give similar results for the radial fluxes, but miss the i-e coupling effect in the deep PS regime.

Kinetic electrons (Fp, no i-e) enhance ion transport by ~ 9%.

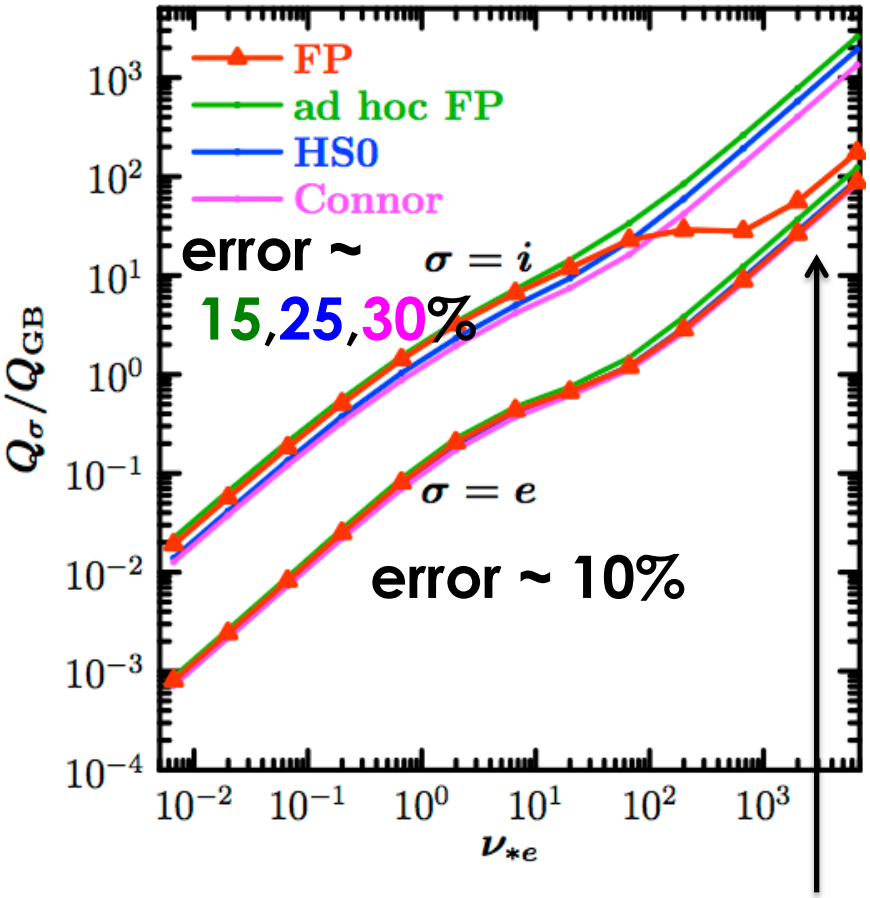

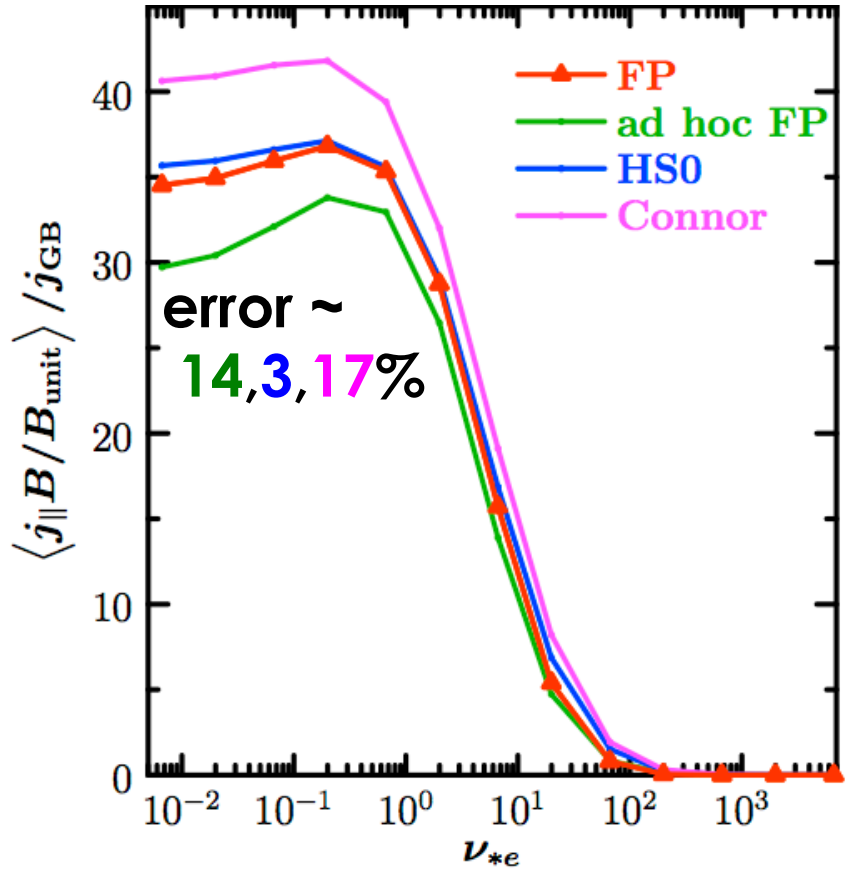

Q_i reduced to Q_e

The (ξ , θ) structure of model operators is similar to the full FP op at low to intermediate collisionality.

ν_{*e}=0.5

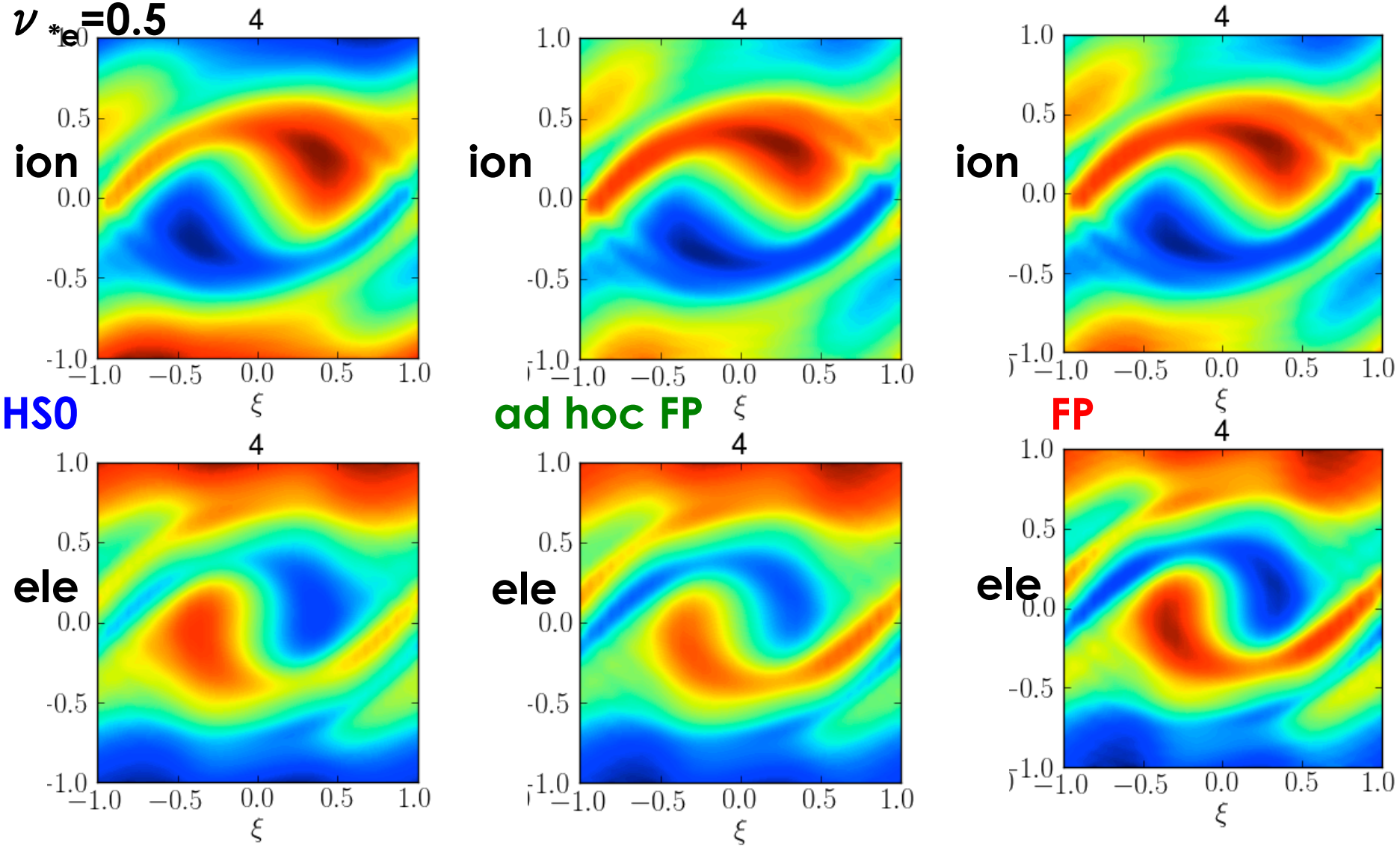

The (ξ , θ) structure of model operators begins to differ from the full FP op at high collisionality.

ν_{*e}=50

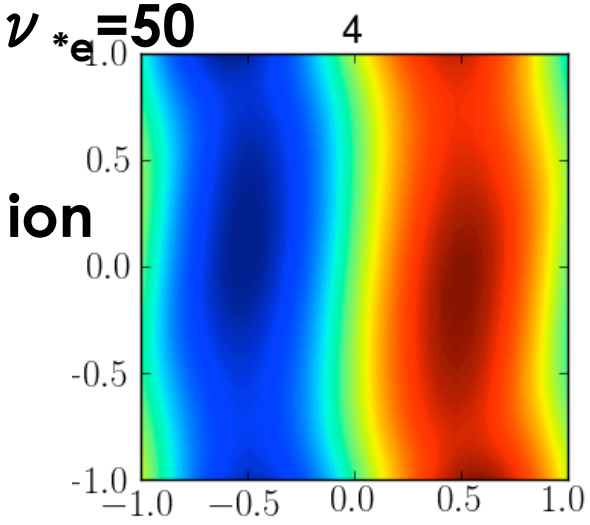

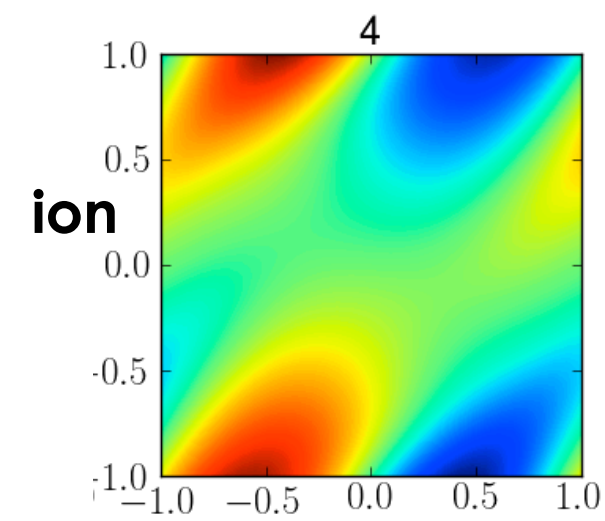

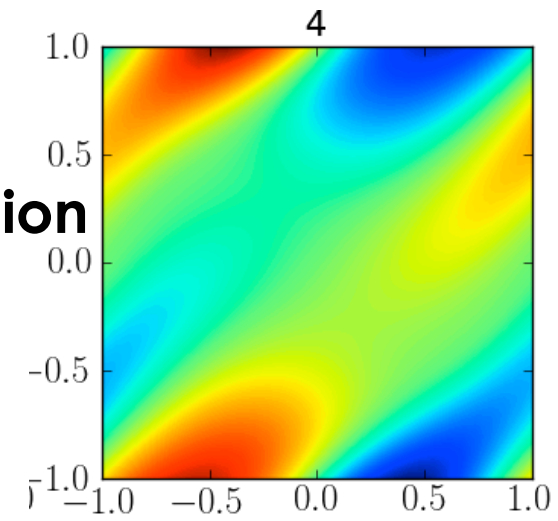

With impurities, numerical simulation is essential since analytic theories are generally quite poor.

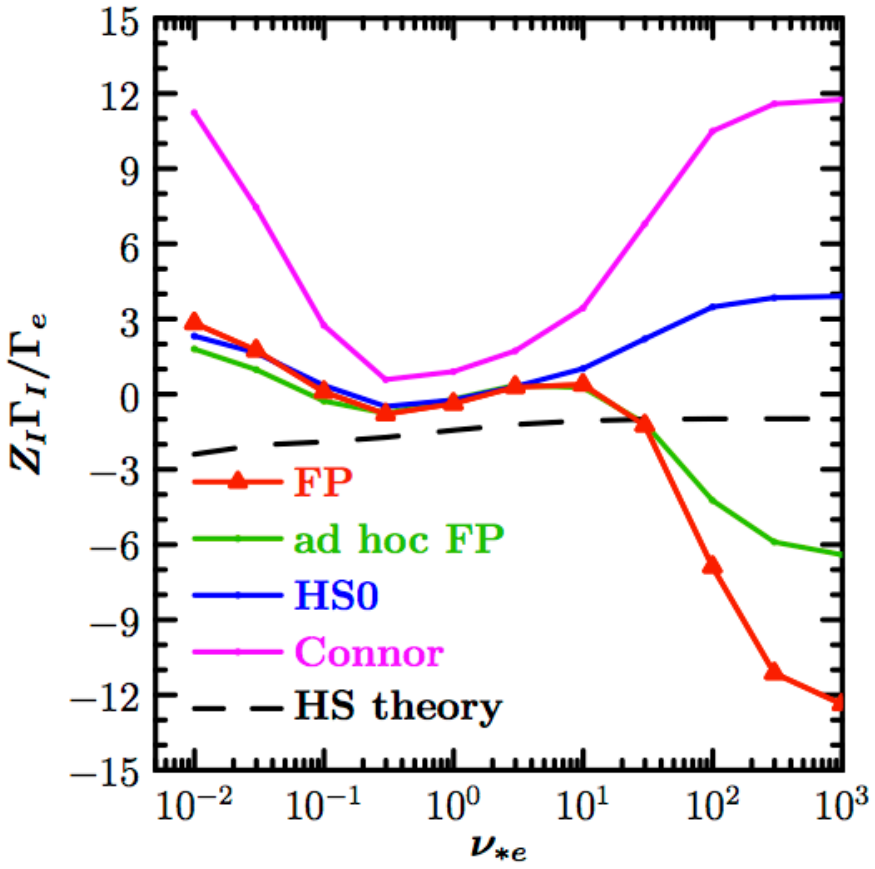

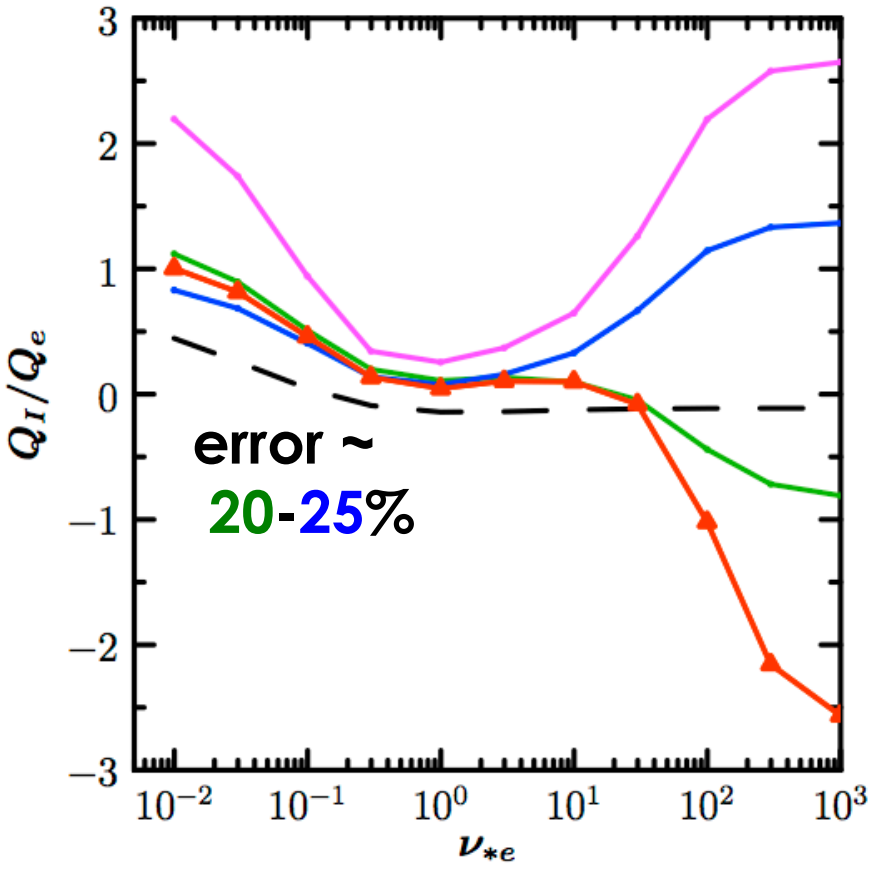

The Connor model is largely inaccurate since it does not model the deceleration effect.

Outline

- **Overview of kinetic theory**
- **Drift-kinetic neoclassical simulations**
  - Numerical algorithms
  - Reduced models
- **Integrated modeling**
  - **MHD equilibrium reconstruction**
  - **Steady-state transport**
- **Advanced physics effects**
  - Strong toroidal rotation
  - Nonaxisymmetry
  - Nonlocal effects

Kinetic equilibrium reconstructions are the first step for accurate transport and stability analysis.

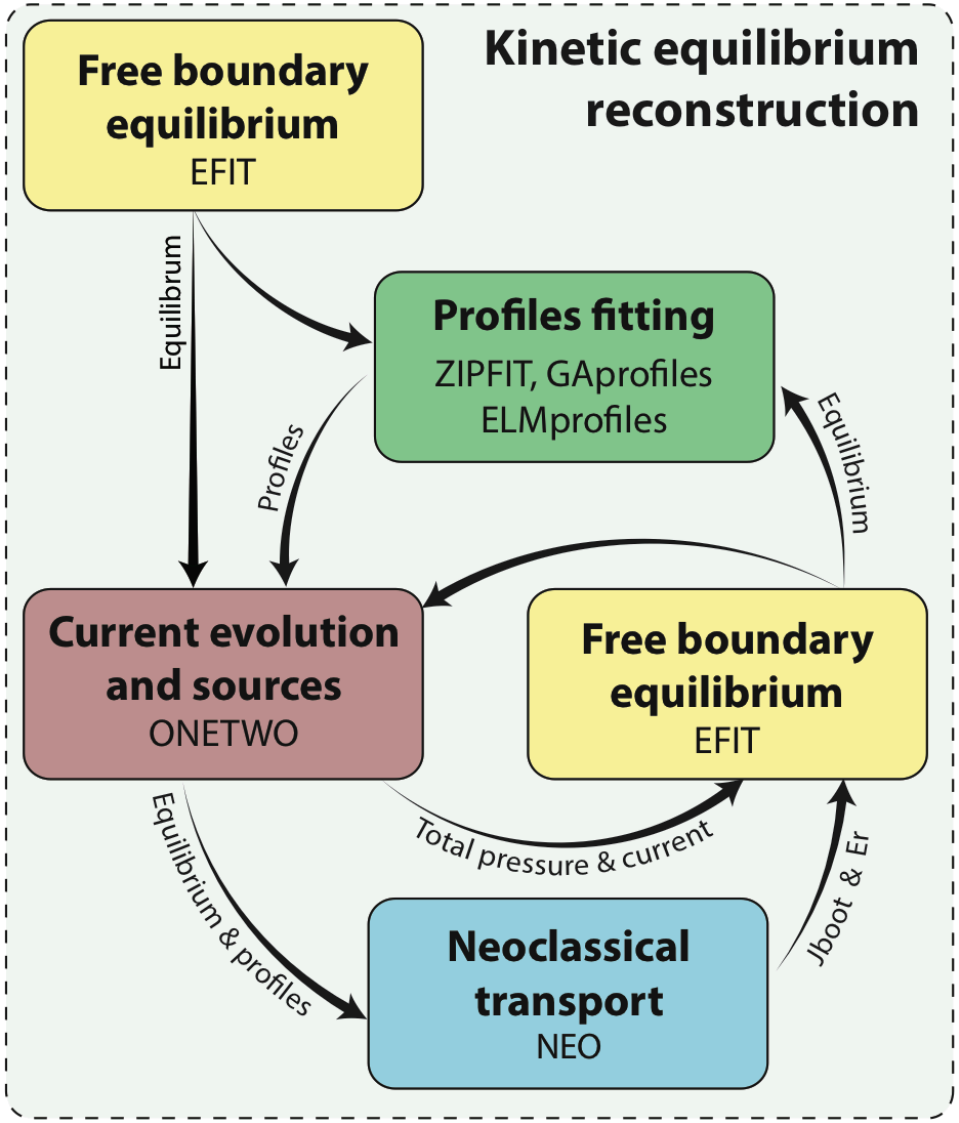

1. Run EFIT using magnetics measurements
2. Fit kinetic profiles in flux space (ZIPPFIT, GAprofiles, ELMprofiles)
3. Run ONETWO transport code to determine sources and fast ion pressure
4. Run kinetic constrained EFIT
5. Run NEO to get accurate predictions of J_{BS} and E_r
6. Repeat 2-5 with updated equilibrium

Fig from O. Meneghini, ATOM, 2014

Analytic models of bootstrap current are often used in analysis, but these have limitations.

shot #	description	ν_{*e}	f_I	$-\frac{\langle j_\parallel B\rangle_{neo}}{B_{unit}}$ (MA/m^2)	$1-\frac{\langle j_\parallel B\rangle_{sauter}}{\langle j_\parallel B\rangle_{neo}}$ (%)
149220	QH-mode	0.068	0.62	0.399	4.7%
145098	QH-mode	0.092	0.26	0.373	2.6%
145421	H-mode	0.398	0.25	0.360	1.7%
144987	H-mode	1.297	0.058	0.184	-20.3%
144977	H-mode	1.383	0.046	0.287	-18.4%
144981	H-mode	2.434	0.034	0.255	-32.4%
145701	H-mode	4.202	0.11	0.070	-49.5%

DIII-D #145419

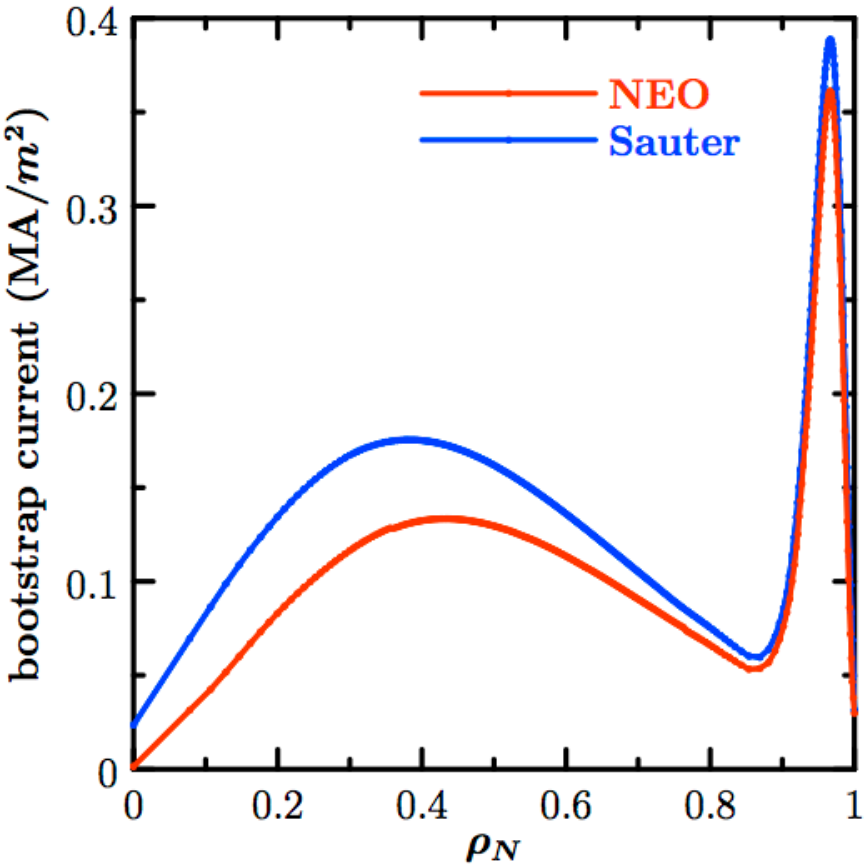

The correction of NEO to Sauter in the pedestal implies that it could significantly improve the accuracy of P-B and KBM calculations.

Integrated modeling of MHD equilibrium reconstruction which couples NEO with kinetic EFIT finds that the current constraint from NEO is more consistent with the pressure and magnetic measurements.

DIII-D #145701

Total edge current profile

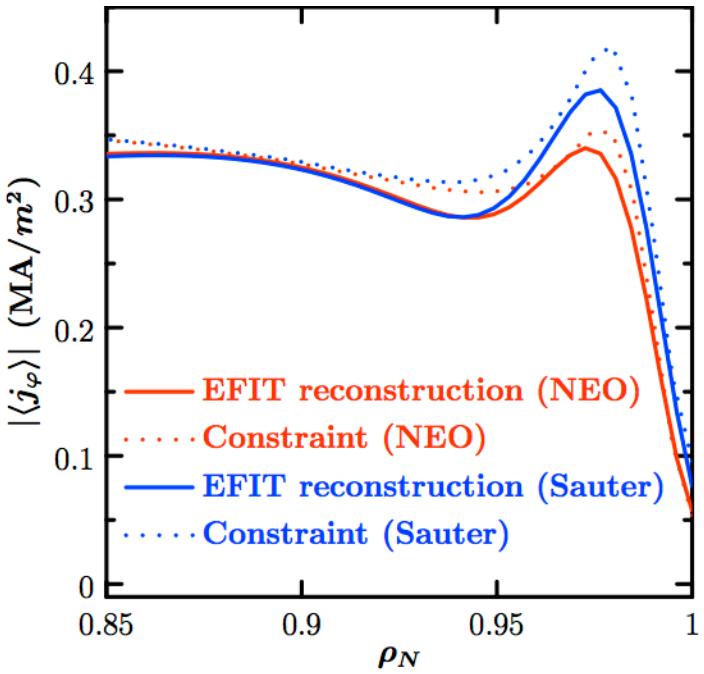

Square Root of Toroidal Flux

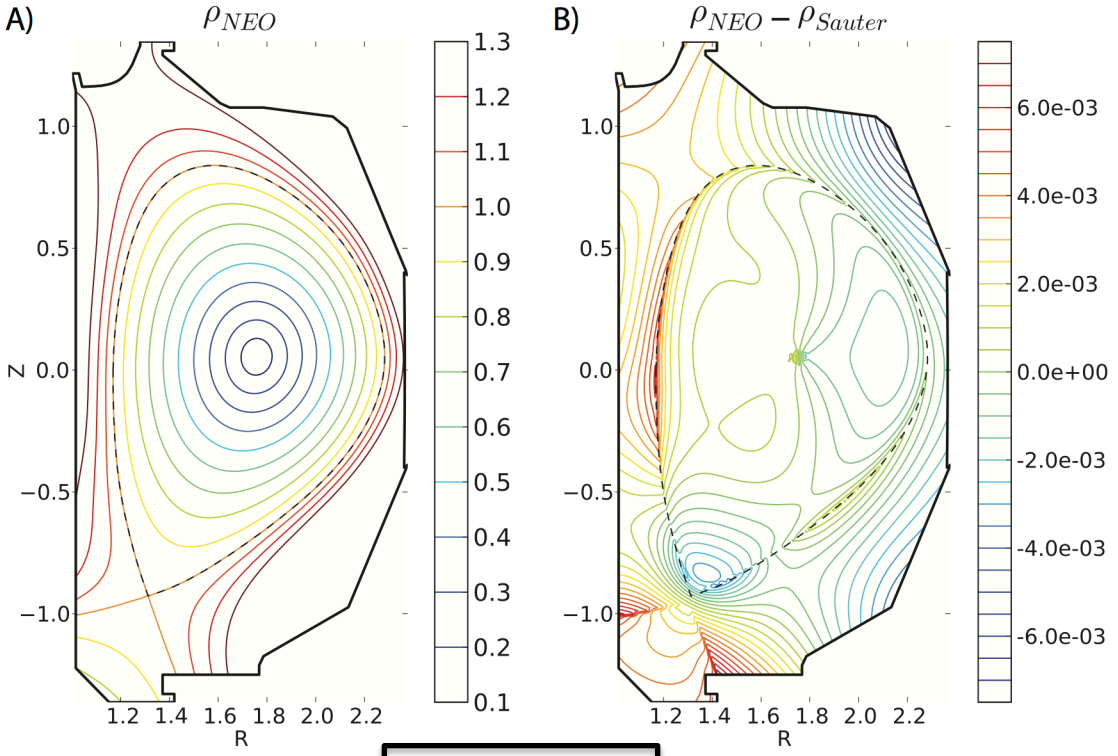

$$\chi^2_{neo} = 64.1$$
$$\chi^2_{sauter} = 85.0$$

Investigation of peeling-ballooning stability can lead to improved understanding of constraints on pedestal height and the mechanism for ELMs.

- **VARYPED**
  - Produces a series of EFITS with a variation in pedestal params
- **ELITE**
  - 2D eigenvalue code based on an ideal MHD generalization of ballooning theory

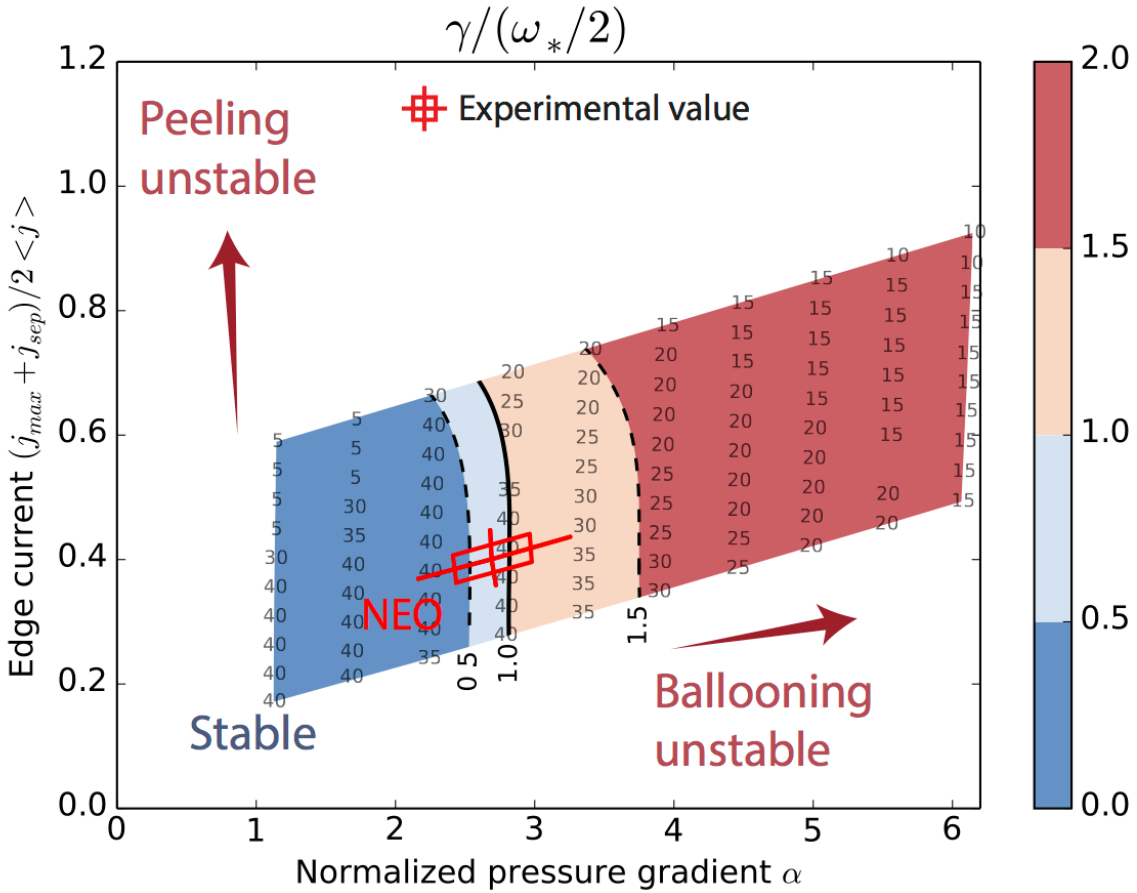

Outline

- **Overview of kinetic theory**
- **Drift-kinetic neoclassical simulations**
  - Numerical algorithms
  - Reduced models
- **Integrated modeling**
  - **MHD equilibrium reconstruction**
  - **Steady-state transport**
- **Advanced physics effects**
  - Strong toroidal rotation
  - Nonaxisymmetry
  - Nonlocal effects

Steady-state transport codes like TGYRO provide an integrated solution of the Fokker-Planck hierarchy.

Obtain steady-state profiles of $n_a(r)$, $T_a(r)$, $\omega_0(r)$ that drive fluxes that balance specified input power

$$\frac{\partial \langle n_a \rangle}{\partial t} + \frac{1}{V'}\frac{\partial}{\partial r}\left(V'\Gamma_a\right) = S_{na}$$

$$\frac{3}{2}\frac{\partial \langle n_a T_a \rangle}{\partial t} + \frac{1}{V'}\frac{\partial}{\partial r}\left(V'Q_a\right) + \Pi_a \frac{\partial \omega_0}{\partial \psi} = S_{Wa}$$

$$\frac{\partial}{\partial t}\left(\omega_0 \langle R^2 \rangle \sum_a m_a n_a\right) + \frac{1}{V'}\frac{\partial}{\partial r}\left(V'\sum_a \Pi_a\right) = \sum_a S_{\omega a}$$

$$\Gamma_a = \Gamma_a^{GV} + \Gamma_a^{neo} + \Gamma_a^{tur}$$
$$Q_a = Q_a^{GV} + Q_a^{neo} + Q_a^{tur}$$
$$\Pi_a = \Pi_a^{GV} + \Pi_a^{neo} + \Pi_a^{tur}$$

Nonlinear root-finding problem:

- Given initial profiles and choose radial pivot point
- Calculate fluxes using **NEO**+**GYRO** at each radius $\{r_j\}$, $0 < r_j \leq r_{max} < a$
- Adjust profiles until **NEO**+**GYRO** fluxes balance sources

For the turbulence flux calculations, TGYRO uses GYRO.

- Nonlinear gyrokinetic solver
- Local (flux tube) or global radial domain
- Fully electromagnetic, realistic shaped geometry, collisions, ExB rotation, parallel velocity shear
- Hybrid parallelization (MPI + OpenMP)

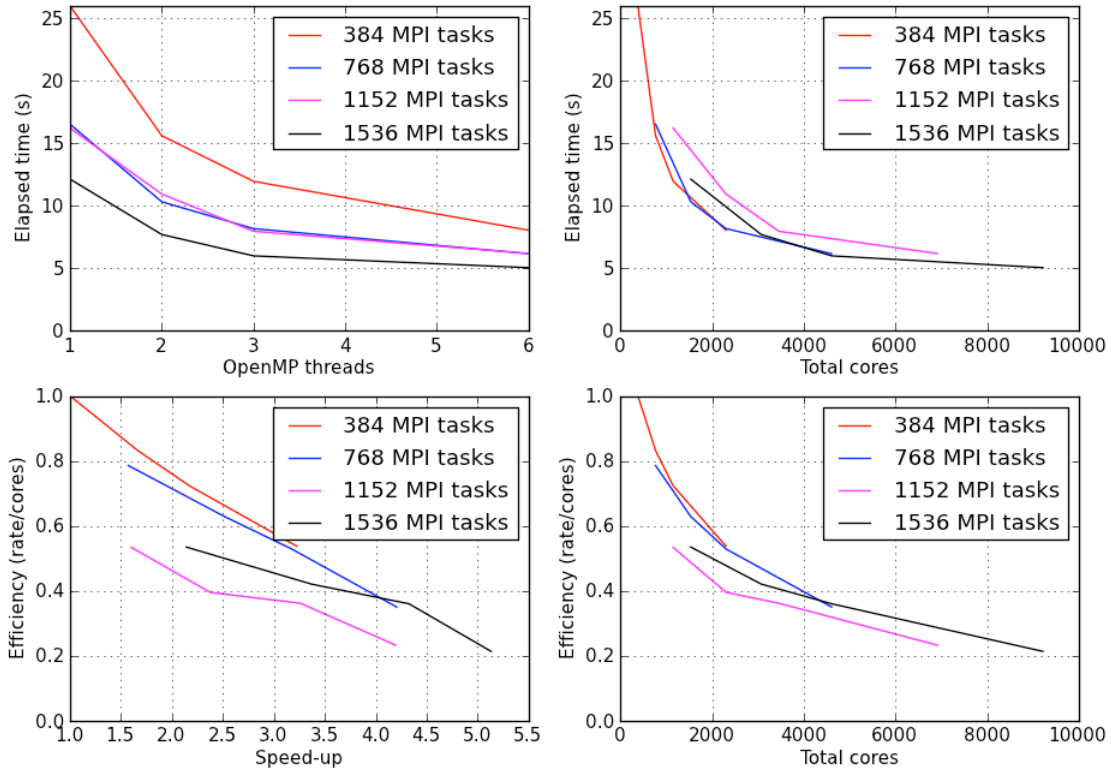

TGYRO manages iterative calls of GYRO for the turbulent fluxes and NEO for the neoclassical fluxes.

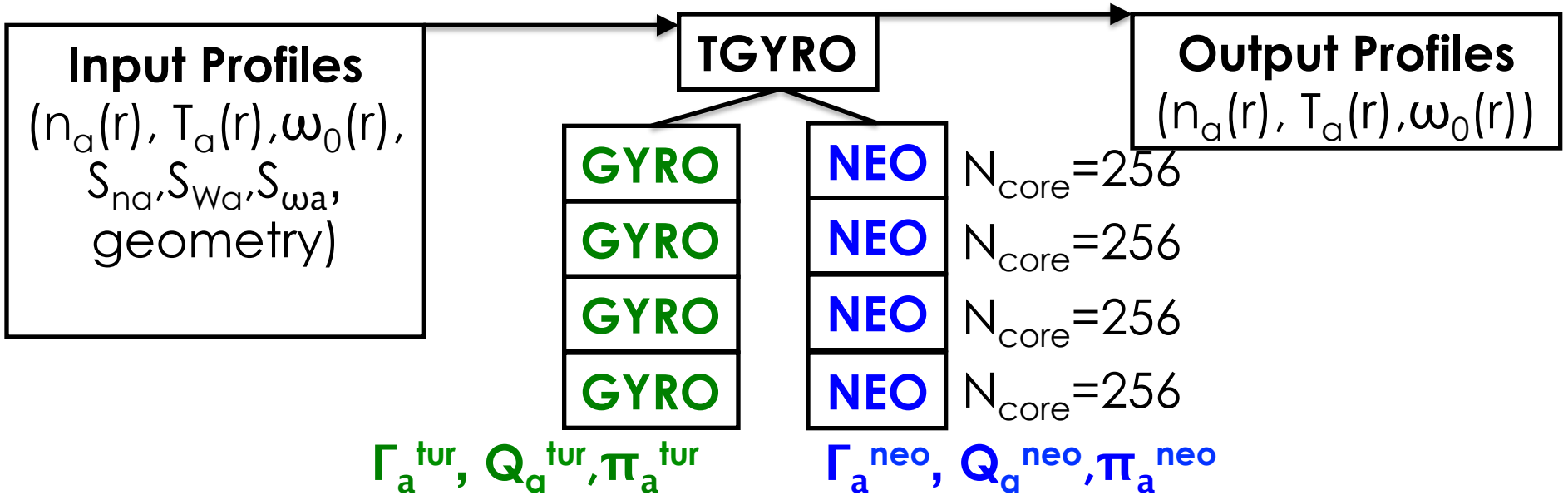

Resource Requirements: 24+ hours on 10,000 cores

TGYRO compares well with fits to experimental data.

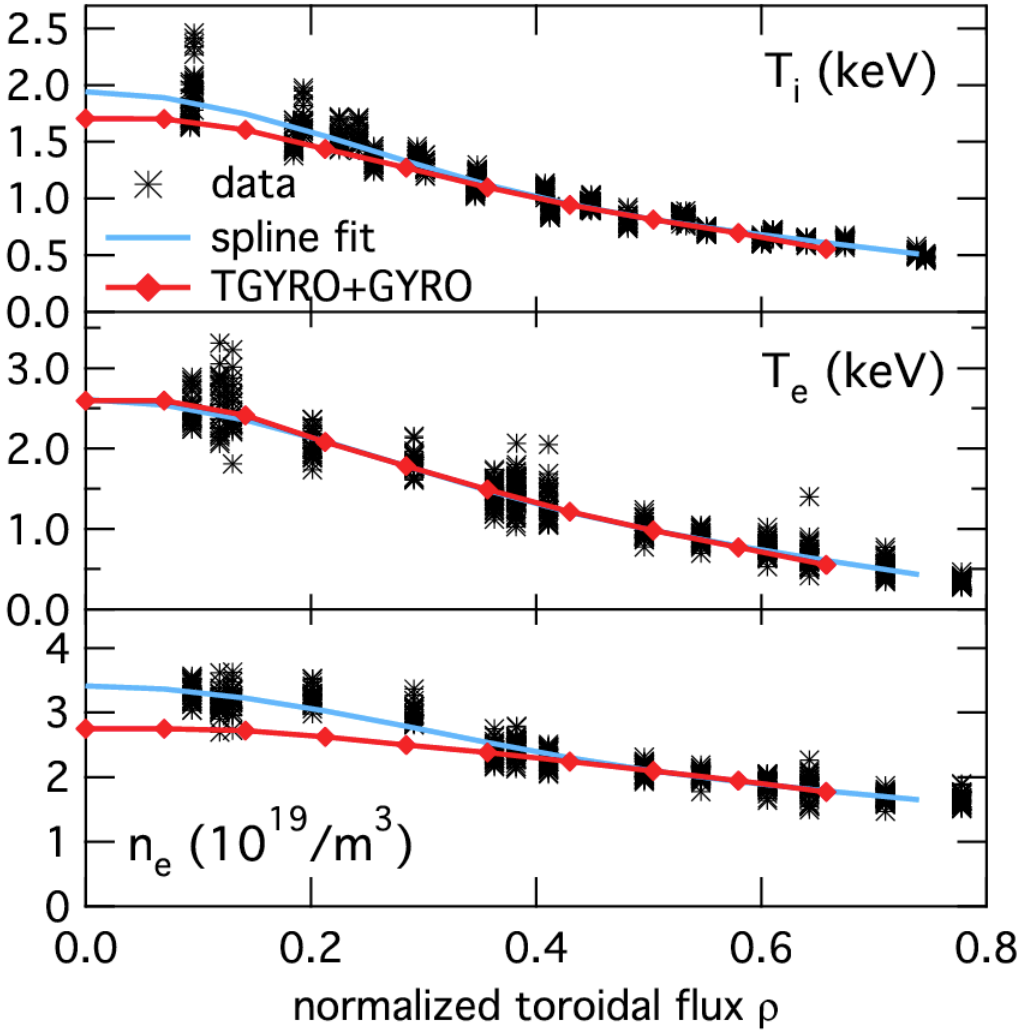

Fig from J. Candy, POP, 2009

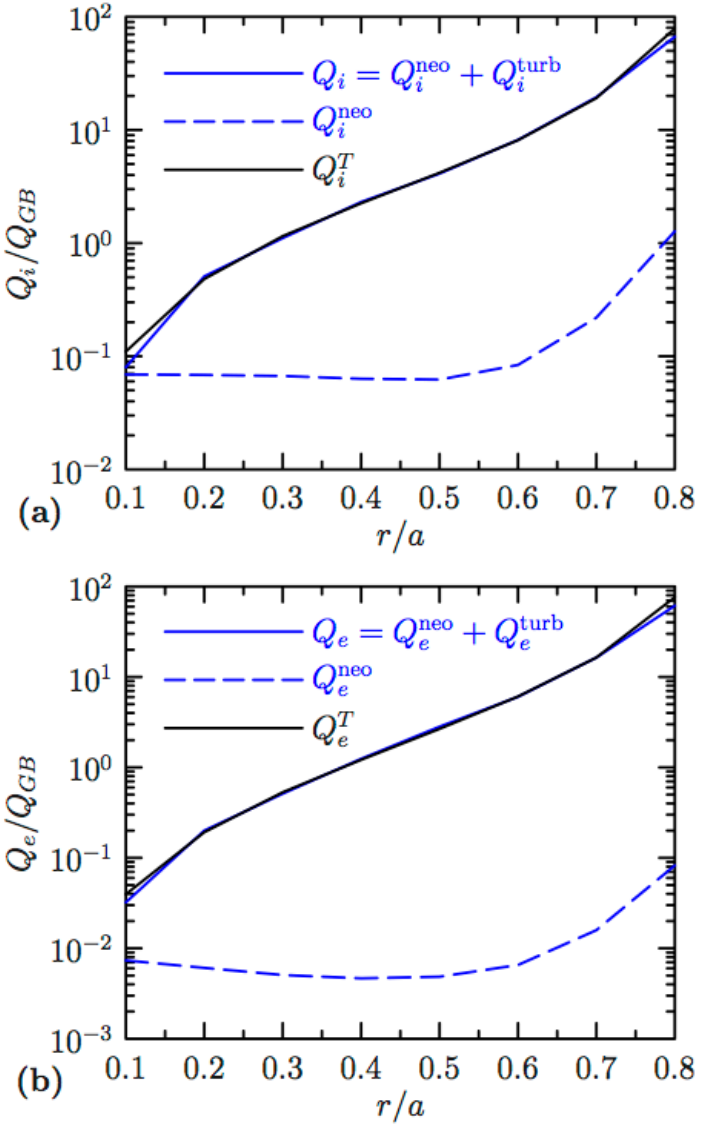

Complete predictive transport modeling involves iterating between kinetic EFIT and TGYRO.

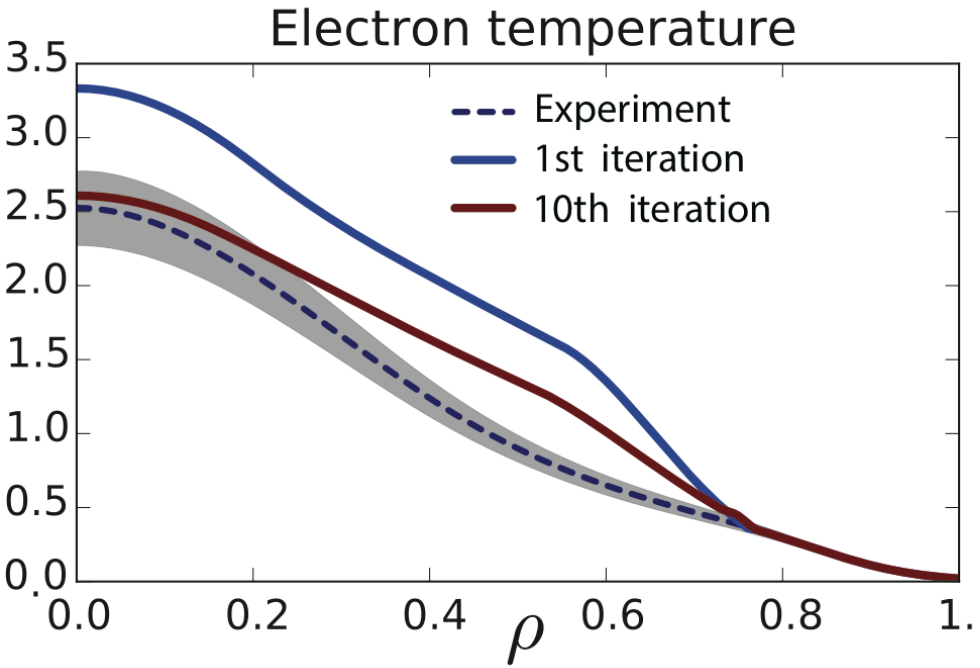

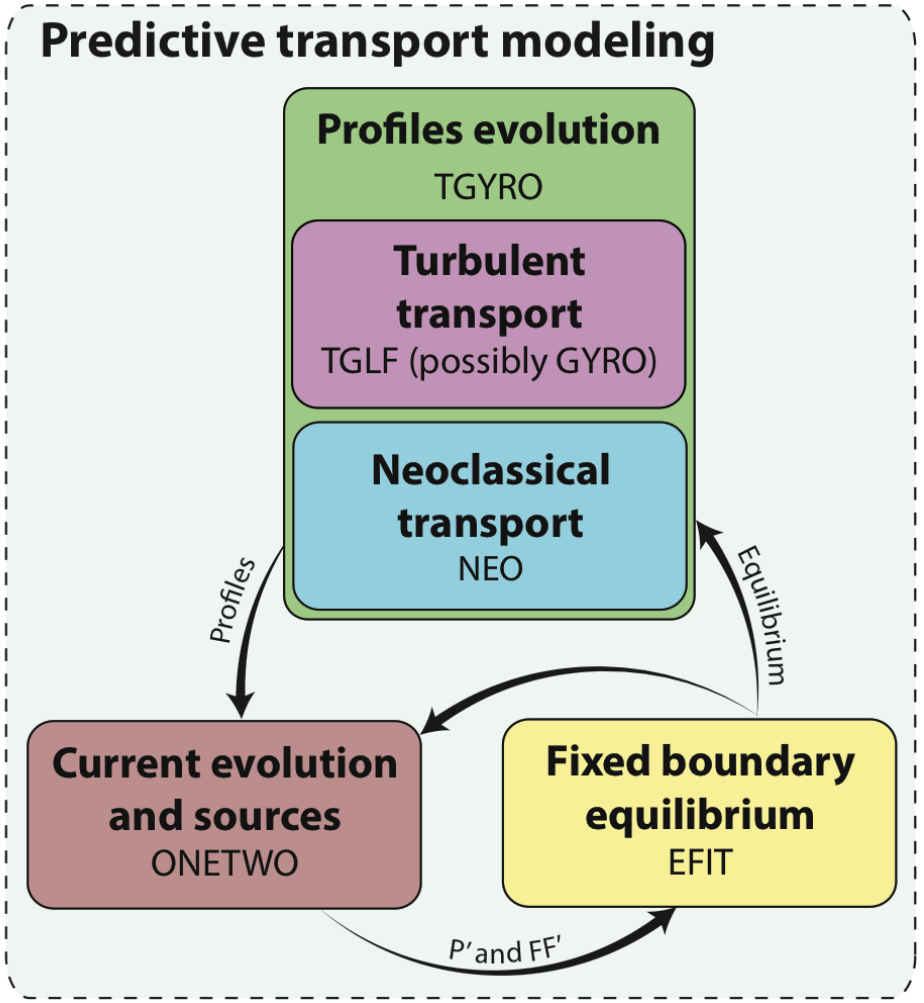

Fig from O. Meneghini, ATOM, 2014

Outline

- **Overview of kinetic theory**
- **Drift-kinetic neoclassical simulations**
  - Numerical algorithms
  - Reduced models
- **Integrated modeling**
  - MHD equilibrium reconstruction
  - Steady-state transport
- **Advanced physics effects**
  - **Strong toroidal rotation**
  - **Nonaxisymmetry**
  - **Nonlocal effects**

Strong toroidal rotation can arise in tokamaks from torque due to NBI and can significantly affect heavy impurity transport.

- The **centrifugal force** pushes the ions toroidally outward, causing them to redistribute non-uniformly around a flux surface.

- As a result of QN, a **poloidally-varying** Φ is generated to balance the density asymmetry.
  - Banana: **increases effective trapped particle fraction**
  - Pfirsch-Schluter: **increases effective toroidal curvature**

- Cannot be studied with a fluid/moment code

To study this, we use extended drift-ordered transport theory which allows for flow speeds ~ O(v_{th}).

Lowest-order constraint:

$$\Phi = \Phi_{-1} + \Phi_0 + \Phi_1 + \Phi_2 + \ldots$$

$$\vec{V}_{0a} = \omega_0 R^2 \nabla\varphi \quad , \quad \omega_0(\psi) = -cd\Phi_{-1}/d\psi$$

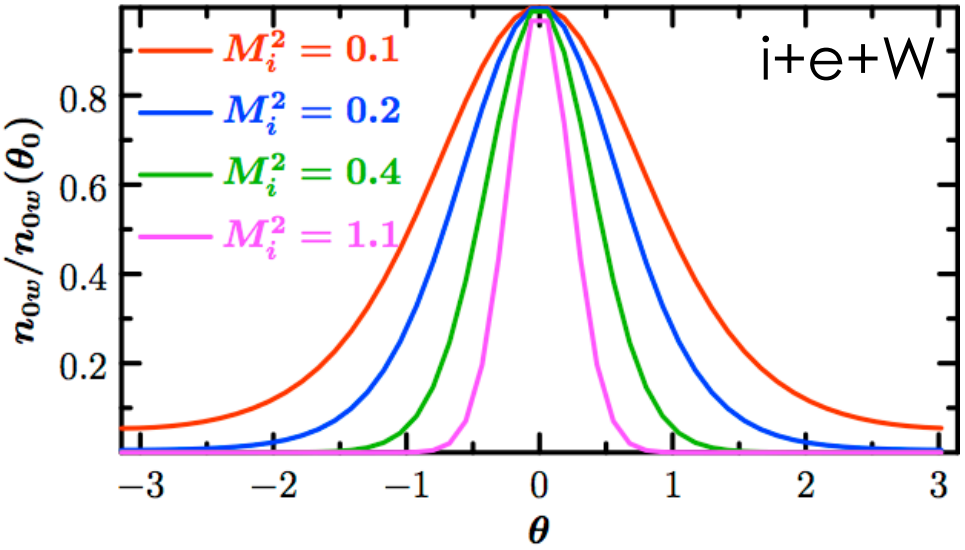

O(1) : $v_{\|}\hat{b}\cdot\nabla f_{0a} = C_{aa}(f_{0a}, f_{0a})$

$$f_{0a} = \frac{n_{0a}(\psi,\theta)}{(2\pi T_{0a}/m_a)^{3/2}} \exp\left(-v^2/\left(2v_{ta}^2\right)\right)$$

$$n_{0a}(\psi,\theta) = N_{0a}(\psi)e^{-\lambda_a(\psi,\theta)}$$

$$\lambda_a(\psi,\theta) = \frac{z_a e}{T_{0a}}\left(\Phi_0 - \langle\Phi_0\rangle\right) - \omega_0^2 R^2(\theta)/\left(2v_{ta}^2\right)$$

$$\tilde{\Phi}_0 = \Phi_0 - \langle\Phi_0\rangle \quad \rightarrow \quad \sum_a z_a e n_{0a}(\psi,\theta) = 0$$

v → rotating frame speed

O(ρ*) : $\frac{\sqrt{2}\mathrm{v}_{ta}\xi}{J_\psi B}\left(x_a\frac{\partial g_{1a}}{\partial\theta} - \frac{1}{2}\frac{\partial\lambda_a}{\partial\theta}\frac{\partial g_{1a}}{\partial x_a}\right) - \frac{1}{\sqrt{2}}\frac{(1-\xi^2)}{J_\psi B}\left(x_a\mathrm{v}_{ta}\frac{1}{B}\frac{\partial B}{\partial\theta} + \frac{\mathrm{v}_{ta}}{x_a}\frac{\partial\lambda_a}{\partial\theta}\right)\frac{\partial g_{1a}}{\partial\xi} - \sum_b C_{ab}^L(f_{1a}, f_{1b})$

$$= -f_{0a}\left[W_a^{(1)}(x_a,\xi,\theta)\left(\frac{d\ln N_{0a}}{dr} + \frac{d\ln T_{0a}}{dr}\left(\lambda_a - \frac{3}{2}\right) + \frac{z_a e}{T_{0a}}\frac{d\langle\Phi_0\rangle}{dr} + x_a^2\frac{d\ln T_{0a}}{dr}\right) + W_a^{(2)}(x_a,\xi,\theta)\frac{R}{\mathrm{v}_{ta}}\frac{d\omega_0}{dr}\right]$$

Strong rotation effects increase the W neoclassical transport for experimental plasma by about a factor of 10.

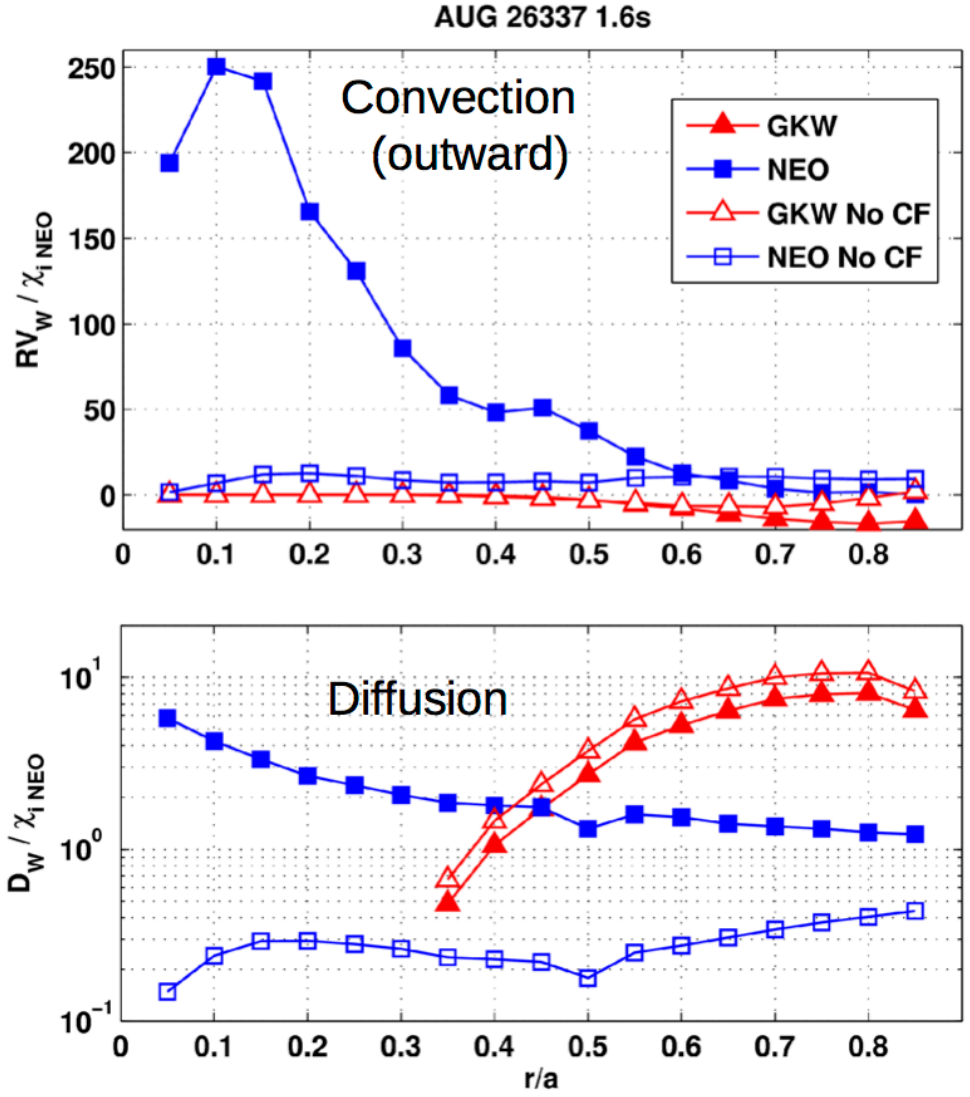

$$\Gamma_W = -D_W \frac{\partial n_{0w}(\theta_0)}{\partial r} + V_W n_{0w}(\theta_0)$$

Fig from F. Casson, EPS, 2014

Qualitative agreement with measurements is seen only if strong rotation effects are included.

SXR tomography (Bremsstrahlung subtracted)

Forward-modeled emission from predicted W distribution (NEO+GKW)

$$\frac{R}{L_{nw}} = -\frac{(\chi_{pb}/\chi_{gkw})RV_{w,gkw} + RV_{W,neo}}{(\chi_{pb}/\chi_{gkw})D_{w,gkw} + D_{W,neo}}$$

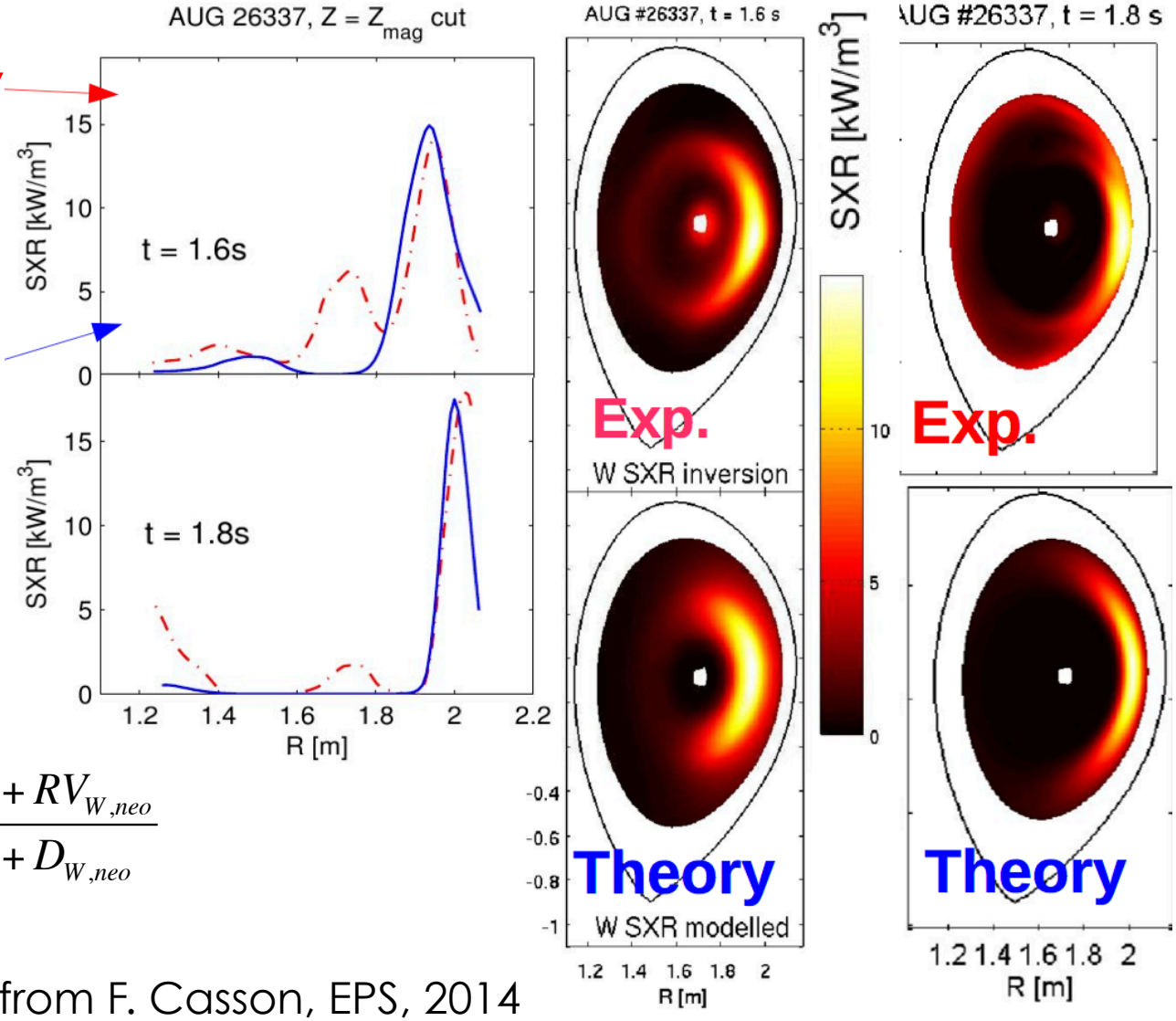

Fig from F. Casson, EPS, 2014

Outline

- **Overview of kinetic theory**
- **Drift-kinetic neoclassical simulations**
  - Numerical algorithms
  - Reduced models
- **Integrated modeling**
  - MHD equilibrium reconstruction
  - Steady-state transport
- **Advanced physics effects**
  - **Strong toroidal rotation**
  - **Nonaxisymmetry**
  - **Nonlocal effects**

Toroidal nonaxisymmetries are always present in tokamaks.

- Caused by magnetic field ripple, imposed resonant magnetic perturbations, MHD activity, etc.

- Can fundamentally change the neoclassical transport since **particles may become trapped in helical magnetic wells**, producing large excursions of particle orbits from the magnetic surface.

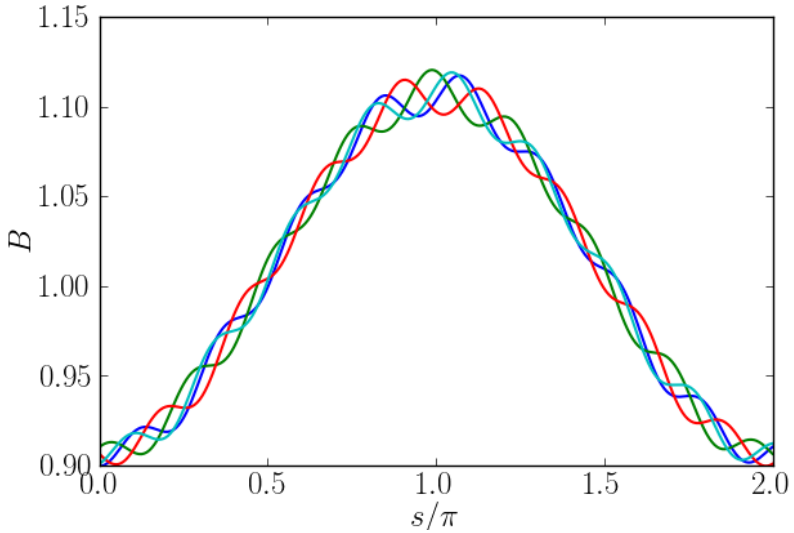

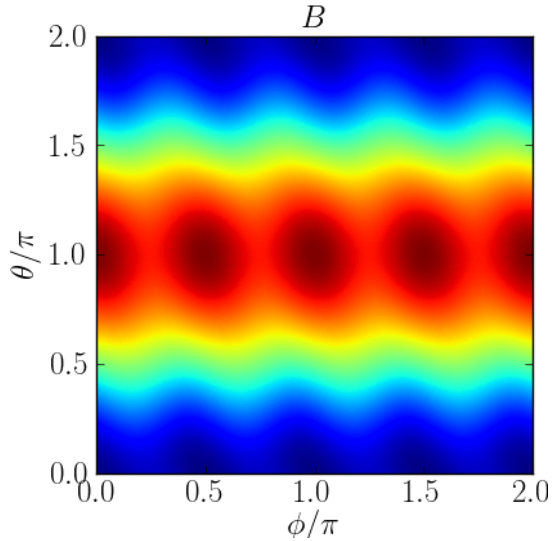

$$R(r,\bar{\theta},\varphi) = R_0 + r\cos\bar{\theta} + \Delta\cos(2\bar{\theta} - 4\varphi) \quad , \quad Z(r,\bar{\theta},\varphi) = r\sin\bar{\theta} + \Delta\sin(2\bar{\theta} - 4\varphi)$$

2D drift-kinetic codes can be generalized to treat general non-axisymmetric equilibria, assuming the existence of flux surfaces.

Solve for $g_{1a}(r,\theta,\varphi,\xi,x_a)$:

$$\sqrt{2}v_{ta}x_a\xi\hat{b}\cdot\nabla g_{1a}-\frac{\sqrt{2}v_{ta}x_a}{2}\frac{\hat{b}\cdot\nabla B}{B}\left(1-\xi^2\right)\frac{\partial g_{1a}}{\partial\xi}-\sum_b C^L_{ab}\left(g_{1a},g_{1b}\right)=-\vec{v}_D\cdot\nabla f_{0a}-f_{0a}\frac{z_a e}{T_a}\vec{v}_D\cdot\nabla\Phi_0$$

$$\rightarrow\quad \Gamma_a=\left\langle\int d^3v g_{1a}\vec{v}_D\cdot\nabla r\right\rangle\ ,\ Q_a=\left\langle\int d^3v g_{1a}T_{0a}x_a^2\vec{v}_D\cdot\nabla r\right\rangle$$

$$u_{\parallel,a}=\left\langle\int d^3v g_{1a}\sqrt{2}v_{ta}x_a\xi/n_{0a}\right\rangle\ ,\ \pi_{t,a}=\left\langle\vec{e}_\varphi\cdot\nabla\cdot\vec{\vec{P}}_a\right\rangle$$

$$\vec{x}=R\sin\varphi\vec{e}_x+R\cos\varphi\vec{e}_y+Z\vec{e}_z$$

$$\vec{B}=\nabla\chi\times\nabla\left(\theta-\iota\varphi\right)=\frac{1}{\sqrt{g}}\left(\frac{\partial\vec{x}}{\partial\varphi}+\iota\frac{\partial\vec{x}}{\partial\theta}\right)$$

$$\sqrt{g}=\frac{\partial\vec{x}}{\partial\chi}\cdot\frac{\partial\vec{x}}{\partial\theta}\times\frac{\partial\vec{x}}{\partial\varphi}$$

$$B=\frac{1}{\sqrt{g}}\left(g_{\varphi\varphi}+\iota^2 g_{\theta\theta}+2\iota g_{\theta\varphi}\right)^{1/2}$$

$$g_{\varphi\varphi}=\frac{\partial\vec{x}}{\partial\varphi}\cdot\frac{\partial\vec{x}}{\partial\varphi}=R^2+\left(\frac{\partial R}{\partial\varphi}\right)^2+\left(\frac{\partial Z}{\partial\varphi}\right)^2$$

$$\hat{b}\cdot\nabla=\frac{1}{B\sqrt{g}}\left(\iota\frac{\partial}{\partial\theta}+\frac{\partial}{\partial\varphi}\right)$$

$$g_{\theta\theta}=\frac{\partial\vec{x}}{\partial\theta}\cdot\frac{\partial\vec{x}}{\partial\theta}=\left(\frac{\partial R}{\partial\theta}\right)^2+\left(\frac{\partial Z}{\partial\theta}\right)^2$$

$$\hat{b}\times\nabla B\cdot\nabla r=\frac{1}{g}\left[-\frac{\partial B}{\partial\theta}\left(g_{\varphi\varphi}+\iota g_{\theta\varphi}\right)+\frac{\partial B}{\partial\varphi}\left(g_{\theta\varphi}+\iota g_{\theta\theta}\right)\right]$$

$$g_{\theta\varphi}=\frac{\partial\vec{x}}{\partial\theta}\cdot\frac{\partial\vec{x}}{\partial\varphi}=\frac{\partial R}{\partial\varphi}\frac{\partial R}{\partial\theta}+\frac{\partial Z}{\partial\varphi}\frac{\partial Z}{\partial\theta}$$

NEO uses the same spectral velocity space algorithm, with a new spectral spatial algorithm.

$$g_{1a} = f_{0a} \sum_{l=0}^{N_\xi} \sum_{m=0}^{N_x} \sum_{p=0}^{N_p-1} \hat{g}_{1a}^{lmp} P_l(\xi) L_m^{k(l)+1/2}\left(x_a^2\right) x_a^{k(l)} F_p(\theta,\varphi)$$

$$\hat{g}(\theta,\varphi) = \sum_{p=0}^{N_p-1} \alpha_p F_p(\theta,\varphi)$$

$$N_p = 1 + 4N_\theta N_\varphi + 2\left(N_\theta + N_\varphi\right)$$

$$= \sum_{m=0}^{N_\theta} \sum_{n=0}^{N_\varphi} \left\{ \begin{array}{l} \sin(m\theta)\left[a_{mn}\cos(n\varphi) + b_{mn}\sin(n\varphi)\right] \\ +\cos(m\theta)\left[c_{mn}\cos(n\varphi) + d_{mn}\sin(n\varphi)\right] \end{array} \right\}$$

- **NEO solves an NxN matrix problem, where $N=N_s N_\xi N_x N_p$**
- The LHS matrix is
  - Band-diagonal in ξ (l)
  - Dense in energy (m)
  - **Dense in space (p)**
  - Dense in species (a)

$$\sum_{j=0}^{m} \sum_{j'=0}^{m'} \Lambda_{mj}^{k} \Lambda_{m'j'}^{k'} A_{aa'}^{ll',jj',pp'} \hat{g}_{1a'}^{l'm'p'} = -\sum_{j=0}^{m} \Lambda_{mj}^{k} S_a^{ljp}$$

Including kinetic electrons and full FP collisions, we identify collisionality regimes of 3D transport.

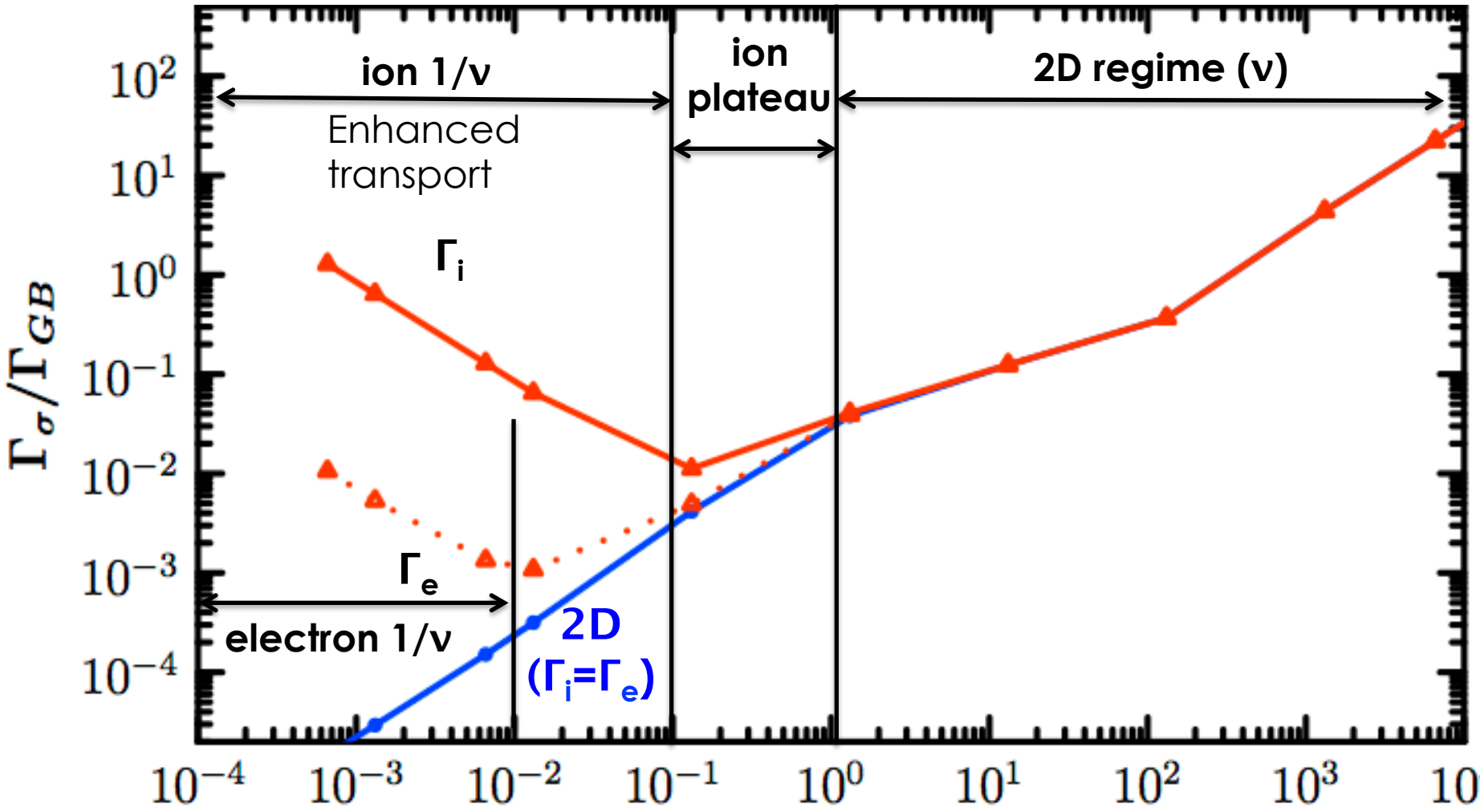

$$\{R,Z\}=\{R_o,0\}+r\{\cos,\sin\}\bar{\theta}+\Delta\{\cos,\sin\}(2\bar{\theta}-4\varphi)$$

Addition of the ExB drift velocity regularizes the unphysical low-ν divergence but is ad hoc and non-rigorous.

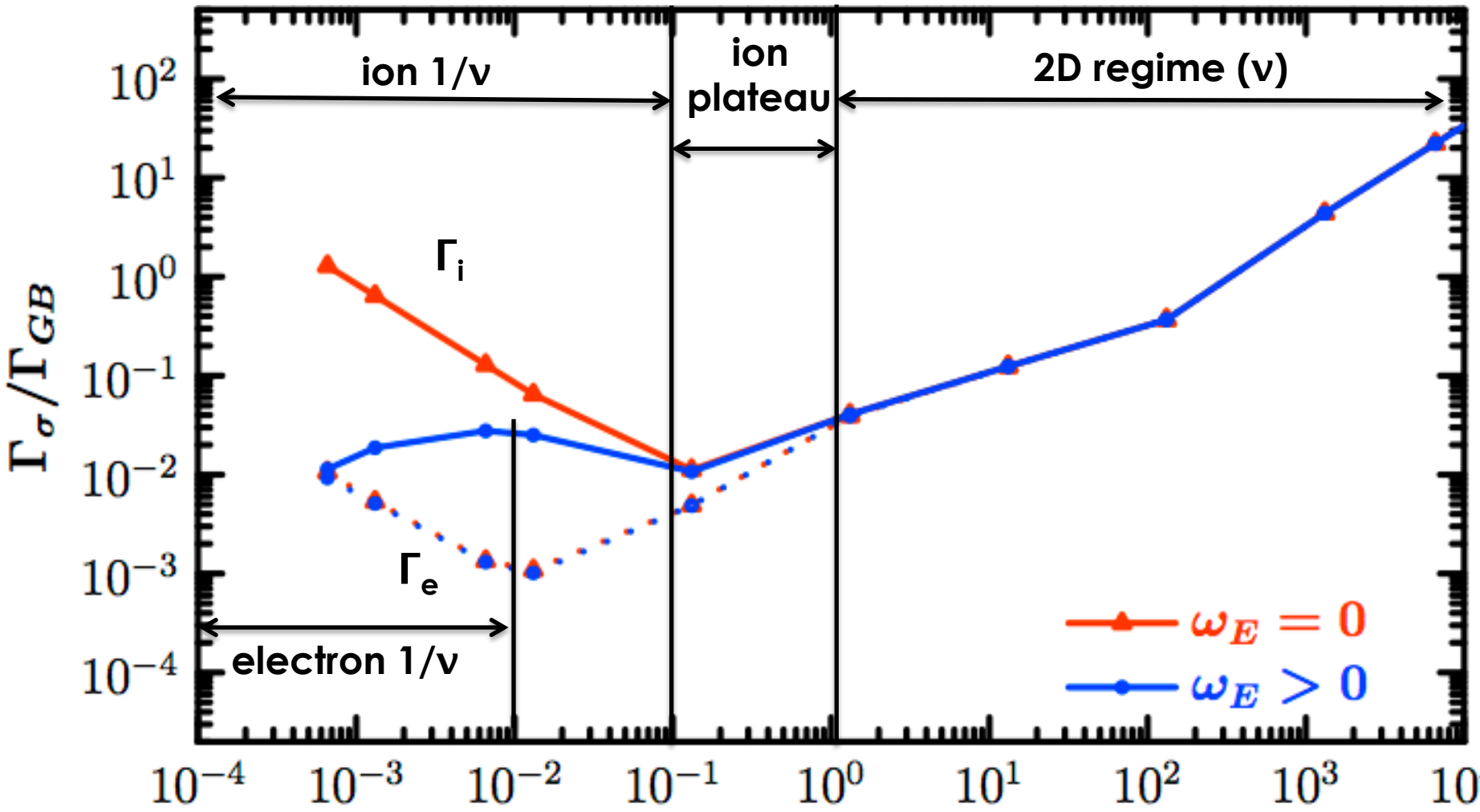

$$\{R,Z\} = \{R_o,0\} + r\{\cos,\sin\}\bar{\theta} + \Delta\{\cos,\sin\}(2\bar{\theta} - 4\varphi)$$

Outline

- **Overview of kinetic theory**
- **Drift-kinetic neoclassical simulations**
  - Numerical algorithms
  - Reduced models
- **Integrated modeling**
  - MHD equilibrium reconstruction
  - Steady-state transport
- **Advanced physics effects**
  - **Strong toroidal rotation**
  - **Nonaxisymmetry**
  - **Nonlocal effects**

The transport becomes nonlocal when the orbit width becomes comparable to or larger than the equilibrium length scale.

Near the magnetic axis

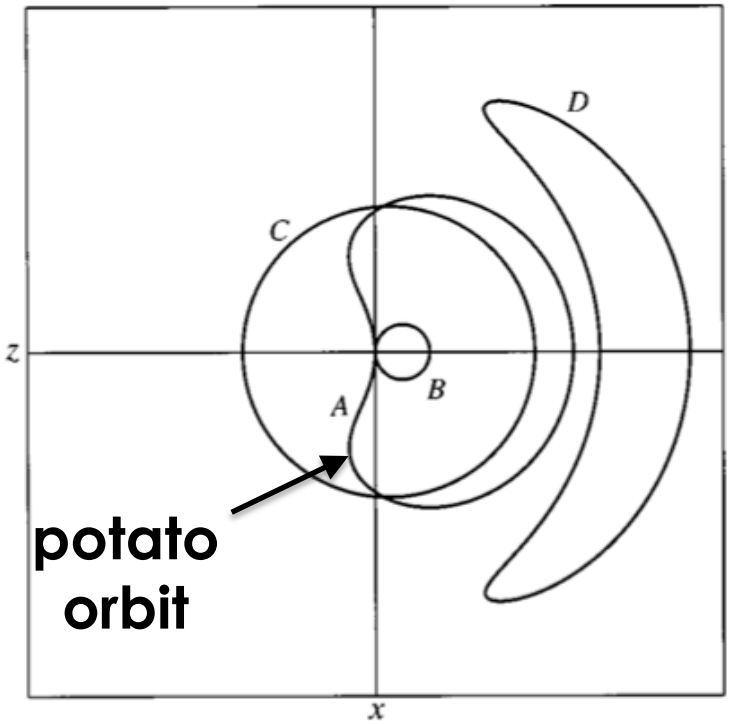

$$r_{potato} = 1.6\left(8q^2\rho_0^2 R_0\right)^{1/3}$$

In regions of steep gradients (ITBs, H-mode pedestal)

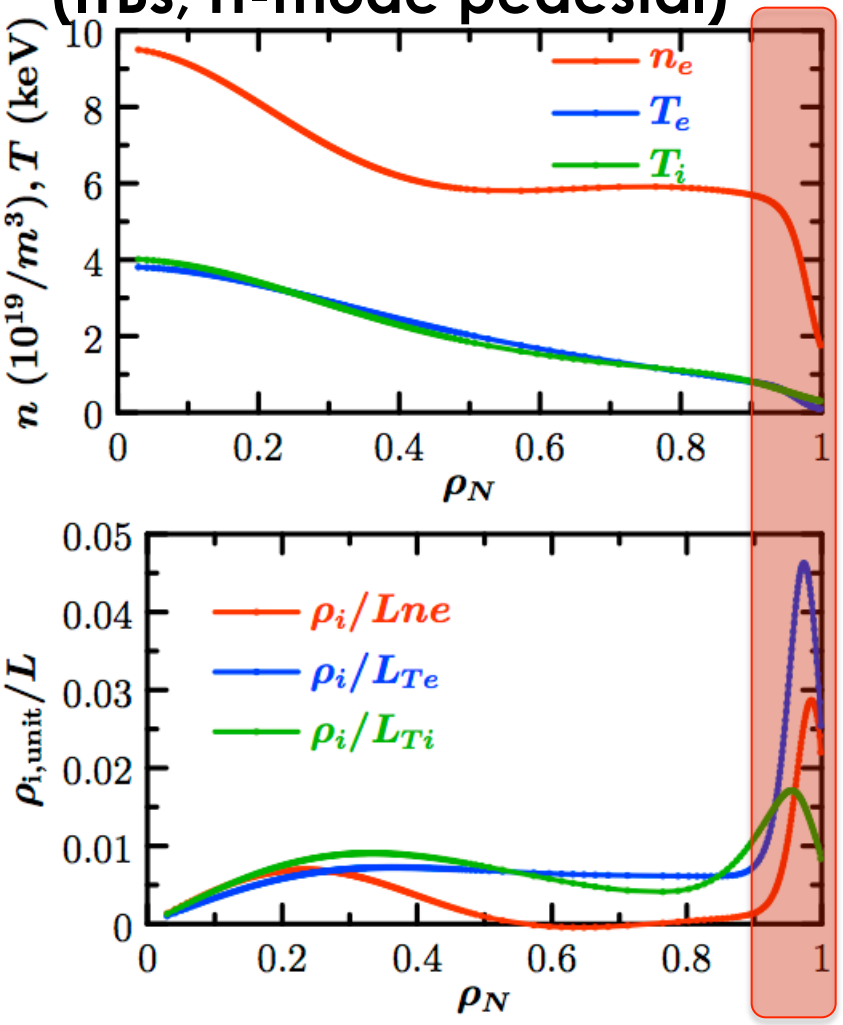

Fig from P. Helander, POP, 7, 2878, 2000

Various mathematical attempts to treat nonlocal neoclassical physics based solely on the DKE are unphysical.

- **The drift-ordering is needed to separate neoclassical transport from gyrokinetics.**
  - **Hazeltine "Full-F DKE"** is obtained by artificially setting **D_a=0**.

$$A=\left[\frac{\partial}{\partial t}+\vec{v}\cdot\nabla+\frac{z_a e}{m_a}\left(\vec{E}+\frac{\vec{v}}{c}\times\vec{B}\right)\cdot\frac{\partial}{\partial\vec{v}}\right]f_a-\left\langle C_a\right\rangle_{ens}-D_a-S_a=0 \quad \rightarrow \textbf{DKE}$$

$$F=\left[\frac{\partial}{\partial t}+\vec{v}\cdot\nabla+\frac{z_a e}{m_a}\left(\vec{E}+\frac{\vec{v}}{c}\times\vec{B}\right)\cdot\frac{\partial}{\partial\vec{v}}\right]\hat{f}_a+\frac{z_a e}{m_a}\left(\hat{\vec{E}}+\frac{\vec{v}}{c}\times\hat{B}\right)\cdot\frac{\partial}{\partial\vec{v}}\left(f_a+\hat{f}_a\right)-C_a+\left\langle C_a\right\rangle_{ens}+D_a=0$$

$\rightarrow$ **GKE**

$$D_a=-\frac{z_a e}{m_a}\left\langle\left(\left(\hat{\vec{E}}+\frac{\vec{v}}{c}\times\hat{\vec{B}}\right)\cdot\frac{\partial\hat{f}_a}{\partial\vec{v}}\right)\right\rangle_{ens}$$

- **For rigorous treatment, Full-F (neoclassical+turbulence, sources, nonlinear collisions, etc.) is needed.**

$$\frac{DF}{Dt}=C_{NL}\left(F,F\right)+S$$

Higher-order solution (in ρ_*) of the Hazeltine eqn serves as an indicator when the δf perturbative formalism is breaking down.

O(ρ_*) : **Standard neoclassical**

$$v_{\|}\hat{b}\cdot\nabla f_{1a}-\frac{z_a e}{m_a}v_{\|}\hat{b}\cdot\nabla\Phi_1\frac{\partial f_{0a}}{\partial\varepsilon}-\sum_a C_{ab}^{L}\left(f_{1a},f_{1b}\right)=-\vec{v}_D\cdot\nabla f_{0a}+\frac{z_a e}{m_a}\vec{v}_D\cdot\nabla\Phi_0\frac{\partial f_{0a}}{\partial\varepsilon}$$

$$0=\sum_a z_a e\int d^3v f_{1a}$$

$$\rightarrow\Gamma_{2a}=\left\langle\int d^3v\left(f_{0a}\vec{v}_E^{(1)}\cdot\nabla r+f_{1a}\vec{v}_D\cdot\nabla r\right)\right\rangle$$

O(ρ_*^2) : **Finite-orbit-width correction**

$$v_{\|}\hat{b}\cdot\nabla f_{2a}-\frac{z_a e}{m_a}v_{\|}\hat{b}\cdot\nabla\Phi_2\frac{\partial f_{0a}}{\partial\varepsilon}-\sum_a C_{ab}^{L}\left(f_{2a},f_{2b}\right)=-\vec{v}_D\cdot\nabla f_{1a}+\frac{z_a e}{m_a}\vec{v}_D\cdot\nabla\Phi_1\frac{\partial f_{0a}}{\partial\varepsilon}$$

$$+\vec{v}_E^{(0)}\cdot\nabla f_{1a}+\vec{v}_E^{(1)}\cdot\nabla f_{0a}+\frac{z_a e}{m_a}\left(v_{\|}\hat{b}\cdot\nabla\Phi_1+\vec{v}_D\cdot\nabla\Phi_0\right)\frac{\partial f_{1a}}{\partial\varepsilon}+\dot{\mu}\frac{\partial f_{1a}}{\partial\mu}+\sum_a C_{ab}^{NL}\left(f_{1a},f_{1b}\right)+S_{2a}$$

Source (required for solvability)

$$-\sum_a\frac{n_{0a}z_a^2e^2}{T_{0a}}\rho_a^2\left|\nabla r\right|^2\frac{\partial^2\Phi_0}{\partial r^2}=\sum_a z_a e\int d^3v f_{2a}$$

$$\rightarrow\Gamma_{3a}=\left\langle\int d^3v\left(f_{0a}\vec{v}_E^{(2)}\cdot\nabla r+f_{2a}\vec{v}_D\cdot\nabla r+f_{1a}\vec{v}_E^{(1)}\cdot\nabla r\right)\right\rangle$$

Numerical solution of the higher-order DKE

- **Solve the local matrix problem for g_{1a}:**

$$\sum_{j=0}^{m}\sum_{j'=0}^{m'}\Lambda_{mj}^{k}\Lambda_{m'j'}^{k'}A_{aa'}^{ll',jj',ii'}\hat{g}_{1a'}^{l'm'i'}\left(r_{\alpha}\right)=-\sum_{j=0}^{m}\Lambda_{mj}^{k}S_{a}^{lji}$$

- **Use g_{1a} and its spatial derivatives as the source term for the O(ρ_*^2) DKE:**

$$v_{\|}\hat{b}\cdot\nabla g_{2a}-\sum_{a}C_{ab}^{L}\left(g_{2a},g_{2b}\right)=-\vec{v}_{D}\cdot\nabla g_{1a}+S_{2a}\quad,\quad S_{2a}\left(x_{a}\right)=-\frac{1}{2}\int_{-1}^{1}d\xi\left\langle\vec{v}_{D}\cdot\nabla g_{1a}\right\rangle$$

  - Same LHS matrix
  - Radial grid points are determined by Fejer's second quadrature method → spectral accuracy

$$\sum_{j=0}^{m}\sum_{j'=0}^{m'}\Lambda_{mj}^{k}\Lambda_{m'j'}^{k'}A_{aa'}^{ll',jj',ii'}\hat{g}_{2a'}^{l'm'i'}\left(r_{\alpha'}\right)=-\sum_{j=0}^{m}\Lambda_{mj}^{k}\tilde{S}_{aa'}^{ll',jj',ii',\alpha\alpha'}\hat{f}_{1a'}^{l'm'i'\alpha'}$$

- **Recursively solve the form of the O(ρ_*^2) DKE.**

With the physical source, the FOW effect cannot be arbitrarily added to the first-order DKE.

Simple example:

- The **O(ρ_*) DKE** is an **inhomogeneous PDE:**

$$\frac{\partial f_{1a}}{\partial t} + L\left(f_{1a}\right) = -\left(\vec{v}_D \cdot \nabla r\right) f_{0a}$$

- Adding the **FOW terms** yields a **homogeneous eqn** in the total F**:**

$$\frac{\partial f_{1a}}{\partial t} + L\left(f_{1a}\right) + \vec{v}_D \cdot \nabla f_{1a} - S\left(f_{1a}\right) = -\vec{v}_D \cdot \nabla f_{0a}$$

$$\rightarrow \quad \left[\frac{\partial}{\partial t} + L + \vec{v}_D \cdot \nabla - S\right]\left(f_{0a} + f_{1a}\right) = 0$$

Unphysical steady-state solution

$f_{1a}=-f_{0a}$

A break-down of the δf formalism due to FOW effects is seen in the vicinity of the potato radius.

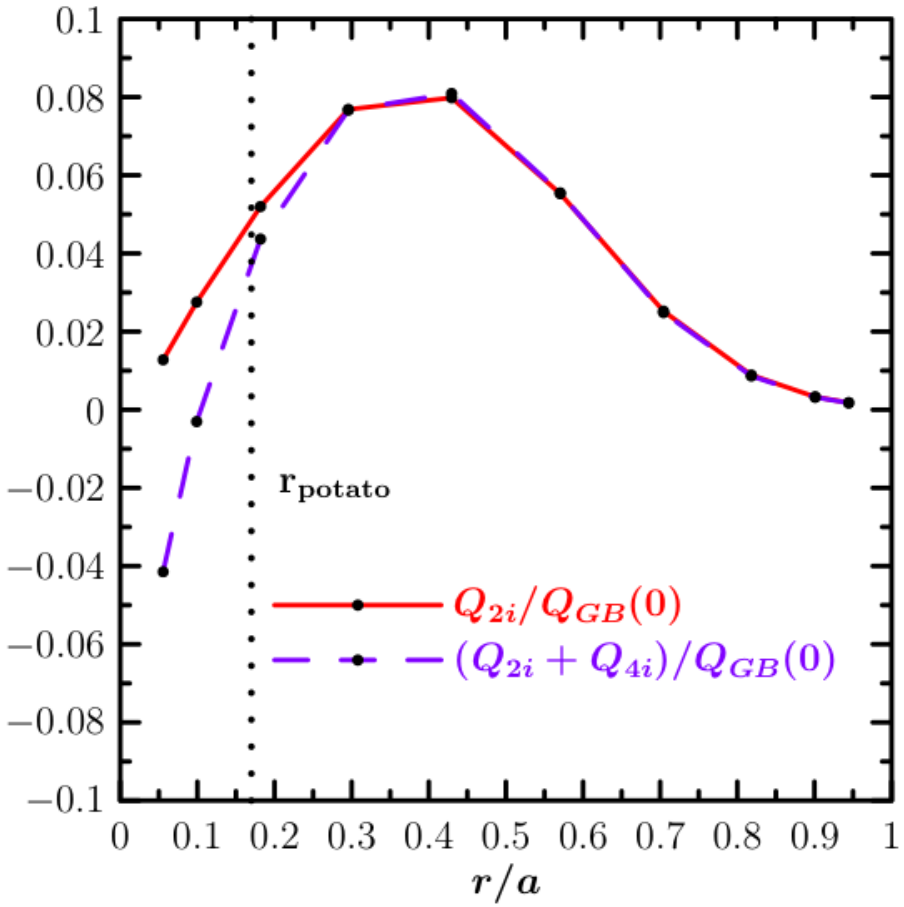

R_0=4 m, a=1m, q=3, B_0=4 T, $(n_{0i},T_{0i}) \sim c_1+c_2\exp(-c_3(r/a)^3)$, s-α geometry, adiabatic ele

For typical DIII-D plasmas, only a weak FOW effect is found due to steep gradients in the H-mode edge.

DIII-D H-mode profiles

shot#132010, t=2.5-3.5s

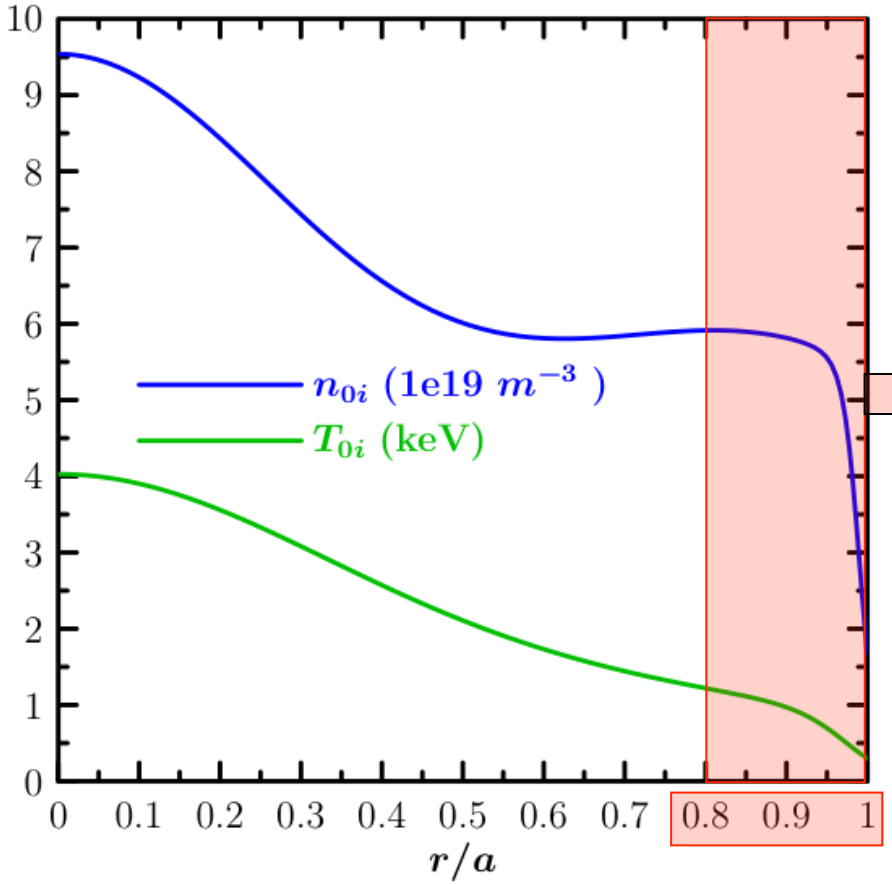

Higher-order NEO results

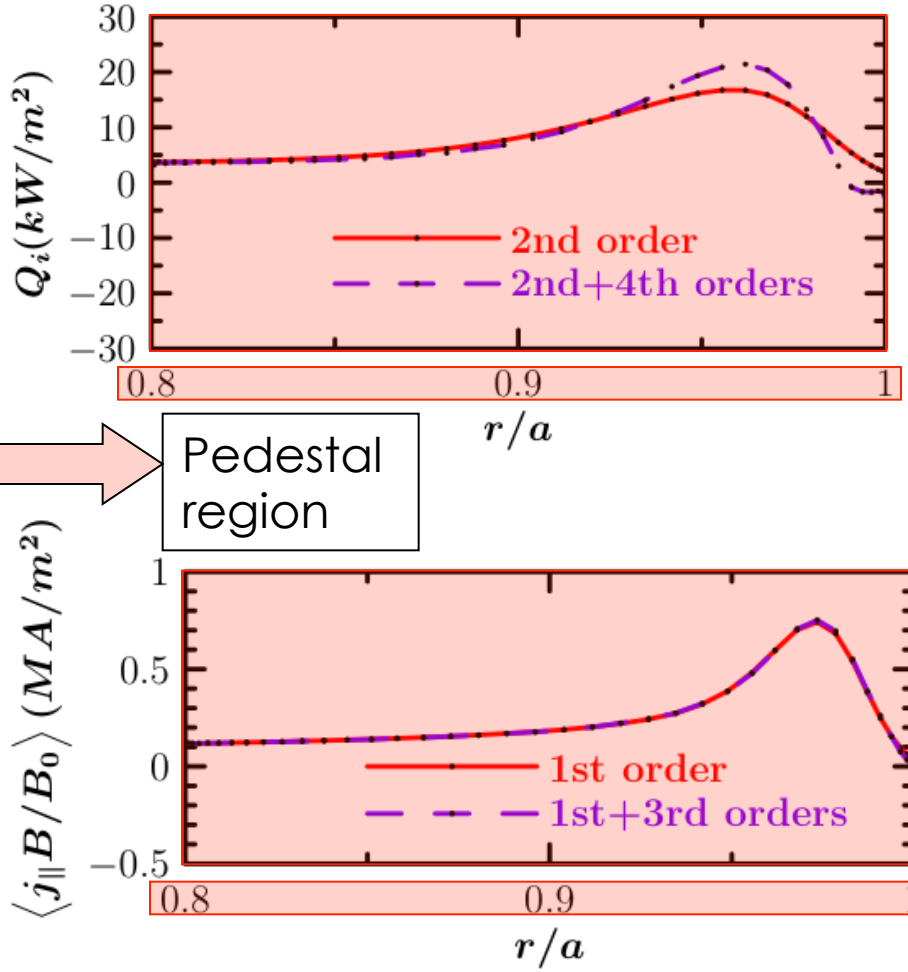

Summary

- **Drift-kinetic simulations** allow for fast, accurate calculations of the neoclassical transport coefficients directly from solution of the distribution functions.
- Unlike gyrokinetics, numerical algorithms are optimized for treatment of the collision dynamics.
- Complete physics requires **full linearized Fokker-Planck collisions**, general geometry, **strong rotation**, and **nonaxsiymmetries**.
- Integrated modeling incorporates:
  - neoclassical bootstrap current into **MHD equilibrium reconstruction** for transport and stability analysis
  - neoclassical fluxes into **steady-state transport calculations**.
- Open questions:
  - Rigorous reduced formulation of transport theory for FOW effects
  - Regularization of transport at low ν in 3D (stochastic motion)
  - Other edge effects (e.g. ion orbit loss), energetic interactions